Air Quality, Atmosphere & Health
https://doi.org/10.1007/s11869-023-01468-0

Drivers of divergent trends in tropospheric ozone hotspots in Spain, 2008–2019

Jordi Massagué[1,2] · Miguel Escudero[3] · Andrés Alastuey[1] · Eliseo Monfort[4] · Gotzon Gangoiti[5] · Hervé Petetin[6] · Carlos Pérez García-Pando[6,7] · Xavier Querol[1]

Received: 5 July 2023 / Accepted: 3 November 2023

Abstract

This study aimed to investigate the causes of contrasting ozone (O_3) trends in Spanish O_3 hotspots between 2008 and 2019, as documented in recent studies. The analysis involved data on key O_3 precursors, such as nitrogen oxides (NOx) and volatile organic compounds (VOCs), among other species, along with meteorological parameters associated with O_3. The dataset comprised ground-level and satellite observations, emissions inventory estimates, and meteorological reanalysis.

The results suggest that the increasing O_3 trends observed in the Madrid area were mostly due to major decreases in NOx emissions from the road transport sector in this urban VOC-limited environment, as well as variations in meteorological parameters conducive to O_3 production. Conversely, the decreasing O_3 trends in the Sevilla area likely resulted from a decrease in NOx emissions in a peculiar urban NOx-limited regime caused by substantial VOC contributions from a large upwind petrochemical area. Unchanged O_3 concentrations in other NOx-limited hotspots may be attributed to the stagnation of emissions from sectors other than road transport, coupled with increased emissions from certain sectors, likely due to the economic recovery from the 2008 financial crisis, and the absence of meteorological variations favorable to O_3 production. In this study, the parameters influencing O_3 varied distinctively across the different hotspots, emphasizing the significance of adopting an independent regional/local approach for O_3 mitigation planning. Overall, our findings provide valuable insights into the causes of contrasting O_3 trends in different regions of Spain, which can be used as a basis for guiding future measures to mitigate O_3 levels.

Keywords Air quality · Tropospheric ozone · Trends · O_3 precursors · Satellite tropospheric NO_2 HCHO · Emissions

✉ Jordi Massagué
jordi.massague@idaea.csic.es

1 Institute of Environmental Assessment and Water Research (IDAEA-CSIC), 08034 Barcelona, Spain

2 Department of Mining, Industrial and ICT Engineering, Universitat Politècnica de Catalunya - BarcelonaTech, (UPC), 08242 Manresa, Spain

3 Department of Applied Physics, School of Engineering and Architecture, Universidad de Zaragoza, 50018 Saragossa, Spain

4 Institute of Ceramic Technology (ITC), Universitat Jaume I, 12006 Castellón, Spain

5 Faculty of Engineering, University of the Basque Country (UPV/EHU), 48013 Bilbao, Spain

6 Barcelona Supercomputing Center (BSC-CNS), 08034 Barcelona, Spain

7 Catalan Institution for Research and Advanced Studies, ICREA, 08010 Barcelona, Spain

Introduction

Tropospheric ozone (O_3) is a key air pollutant that harms human health and the environment, and it is an important greenhouse gas (Fowler et al. 2009; Myhre et al. 2014; GBD 2016; IPCC 2021; WHO 2021, 2013a, b). Additionally, it is a secondary atmospheric pollutant, 90% of which, globally, arises from photochemical reactions in precursors, particularly nitrogen oxides (NOx), volatile organic compounds (VOCs), including methane (CH_4) and carbon monoxide (CO), and the rest from stratospheric contributions (McLinden et al. 2000; Olson et al. 2001; Stevenson et al. 2006; Young et al. 2013). Emissions of the two main O_3 precursors, NOx and VOCs, may have different impacts on ground-level O_3, depending on the local conditions and their relative mixing ratios (Sillman 1999).

NOx-limited conditions tend to occur at locations with low NOx emissions (i.e., rural environments or locations

Published online: 28 November 2023

downwind of urban plumes and large sources) during periods of high photochemical activity, promoting enhanced O_3 formation. Consequently, NOx-limited conditions are often associated with times and locations of high O_3 levels, with increased NOx emissions leading to O_3 increases, while increased VOC emissions may have limited effects (Sillman 1999; Sillman and He 2002; Sillman et al. 2003).

VOC-limited conditions typically occur in areas with high NOx emissions (e.g., urban centers or large pollution plumes) and under conditions of reduced photochemical activity. Such conditions are often associated with lower O_3 levels (i.e., due to NO titration near high NOx emissions and/or low photochemical activity). In VOC-limited conditions, increased NOx emissions can result in localized O_3 decreases, whereas increases in VOC emissions cause increases in O_3 (Jacob et al. 1995; Sillman 1999; Sillman and He 2002; Sillman et al. 2003).

The application of emissions controls on O_3 precursors in Europe, ranging from urban to the national and European scales, has resulted in a varied impact on ground-level O_3. This is a consequence of the spatiotemporal variability of emissions changes in recent decades and the variability of O_3 chemical formation regimes (Monks et al. 2015, Fleming et al. 2018). A review of studies on O_3 trends by Sicard (2021) pointed to a general decrease in O_3 levels in rural European areas from the early 2000s due to effective O_3 precursor emissions control policies. However, these reductions in the precursors were insufficient to transition from VOC-limited to NOx-limited conditions in the cities. Consequently, there has been a general increase in O_3 concentrations in urban environments, underscoring the necessity to apply effective control strategies to VOC emissions. Thus, decreased NOx emissions may to lead to both a reduced number of high O_3 peaks and an increase in the minimum O_3 values. This, in consequence, can lead to a narrowing of the O_3 distribution (Simon et al. 2015), and ultimately drive a convergence between urban and rural O_3 pollution in the long term (Paoletti et al. 2014; Yan et al. 2019). Moreover, at regional background-O_3-monitoring stations, concentrations have increased gradually over the last few decades in the Northern Hemisphere (Sicard 2021). This can likely be attributed to a combination of factors, including the influence of climate change, increased stratospheric O_3 intrusions, increased CH_4 emissions, decreased NO titration due to reduced NOx emissions in production areas, and enhanced hemispheric transport (Monks et al. 2015; Sicard 2021, and related references).

Apart from changes in anthropogenic precursor emissions at the local, regional or global level, O_3 trends are influenced by various interconnected factors, including changes in meteorology (radiation, temperature, transport patterns, etc.), shifts in biogenic emissions, the impacts of biomass burning (regionally and globally), and changes in stratosphere-troposphere exchange, among others (Monks et al. 2015; von Schneidemesser et al. 2015).

The Southern European regions, and especially the Western Mediterranean Basin, are the most exposed to O_3 pollution in Europe, where Spain and several other countries systematically exceed the legal thresholds for the protection of health and vegetation (EEA 2021a).

In a companion study, Massagué et al. (2023) examined the trends in several relevant ground-level O_3 metrics in Spain covering 2008 – 2019. The selected period was framed between two major events that had a substantial impact on global emissions—the 2008 financial crisis and the COVID-19 pandemic in 2020 (Peters et al. 2011; Castellanos and Boersma 2012; Sokhi et al. 2021). The study aimed to classify the atmospheric regions in Spain based on their O_3 pollution patterns and identify the main O_3 hotspots. These included the Madrid region, the interior of the Valencian Community, the northern (downwind) areas of Barcelona, the Guadalquivir Valley, which includes the urban area of Sevilla, and the closed basin of Puertollano.

The O_3 trends in these areas exhibited marked differences: (i) the Madrid region showed the highest number of upward trends across all metrics, often with the highest increasing rates, indicating increasing O_3 levels associated with both chronic and episodic exposure; (ii) the Valencian Community had a mixed variation pattern, depending on the metric considered; (iii) areas situated downwind of Barcelona, the Puertollano Basin, and the Guadalquivir Valley generally did not show O_3 trends, but (iv) the urban area of Sevilla stood out as the only major city in Spain with generalized decreasing O_3 trends.

Building upon this work, in the framework of the development of a Spanish Ozone Mitigation Plan, this study was aimed at exploring possible causes for these contrasting O_3 trends through the analysis of changes in meteorological parameters relevant to O_3 and available information on O_3 precursors.

Methodology

Study area

This study was focused on mainland Spain and the Balearic Islands (Fig. 1a). Figure S1.1 provides general information on the land cover and use, demographics, and main climatic characteristics of the study area. Madrid, Barcelona, Valencia, and Sevilla are the most populated metropolitan areas in Spain. The northern and north-western regions in Spain have the lowest O_3 levels due to meteorological conditions that are not favorable for O_3 production (Gangoiti et al. 2002, 2006; Saavedra et al. 2012) (see Figure S1.1c–f). Conversely, in the central, southern, and Mediterranean areas, O_3 levels tend to

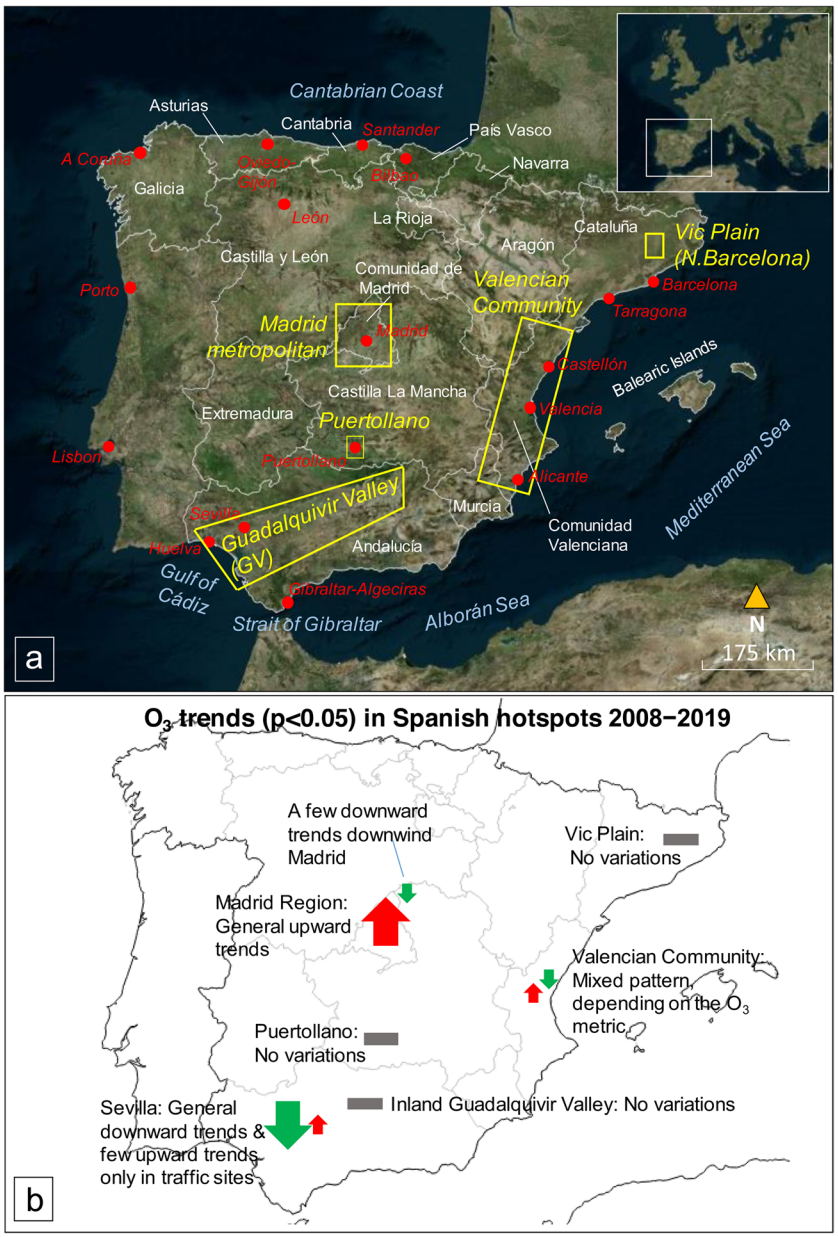

Fig. 1 **a** O_3 hotspots or areas relevant to this study—yellow (fully described in Querol et al. 2016), autonomous regions—white, and important cities mentioned in this study—red. **b** Summary of the main O_3 trends for the main hotspots for 2008–2019 (from Massagué et al. 2023). The size of the arrows provides an indication of the magnitude and number of the trends observed. Upward arrow—O_3 increasing, downward arrow—O_3 decreasing, and gray block—no O_3 variation

be higher due to the occurrence of large anthropogenic and biogenic precursor emissions, the prevailing meteorological conditions during the warm seasons, and the characteristic orography that favors the production and accumulation of O_3 (Millán et al. 1997, 2000; Gangoiti et al. 2001).

The areas frequently impacted by the most intense episodes of O_3 in Spain—or O_3 hotspots (Fig. 1a)—have been described in Diéguez et al. 2009), Querol et al. (2016), and later updated by Massagué et al. (2023). The O_3 phenomenology in these areas has been studied previously—the Madrid metropolitan area (e.g., Plaza et al. 1997; Querol et al. 2018; Reche et al. 2018; Escudero et al. 2019), northern Barcelona (e.g., Toll and Baldasano 2000; Querol et al. 2017; Massagué et al. 2019), the Guadalquivir Valley (e.g., Notario et al. 2012; In 't Veld et al. 2021; Massagué et al. 2021), the Valencian Community, generally including the O_3 dynamics affecting the Western Mediterranean Basin (WMB) (e.g., Millán et al. 1997, 2000; Gangoiti et al. 2001), and the Puertollano Basin (e.g., Saiz-Lopez et al. 2009; Notario et al. 2013).

Figure 1b schematically illustrates the main O_3 trends of the various hotspots during the period 2008 – 2019, as described in the "Introduction" section.

Data and methods

We utilized multiple sources of data, encompassing: (i) concentration data on the available O_3 precursors, including

ground-level measurements of NO_2 and NO, satellite observations of NO_2 and formaldehyde (HCHO) tropospheric columns; (ii) emissions data on the main O_3 precursors, including NOx, VOCs, CO, and CH_4, obtained from official inventories; and (iii) reanalyzed data of several meteorological parameters relevant to O_3. For all data except the emissions data, we considered annual aggregates for the period April to September (i.e., O_3 season), which corresponds to the main vegetation growing season and is when the O_3 levels are typically at their maximum in Europe (EC 2008; Langner et al. 2012; Gaudel et al. 2018; Mills et al. 2018). Additional information can be found in Section S2.

Ground-level concentrations of pollutants

We used NO_2 and NO hourly data series from all the air-quality monitoring stations (AQMSs) in Spain that reported to the European Council based on Decision 2011/850/UE and were active during at least one of the last two years in the study period (2018 or 2019).

Following the same criteria as for the analyses in Massagué et al. (2023), for the assessment of the present-day distribution (2015–2019), each AQMS was required to have had at least three years' worth of valid data for that period, and for the trend estimates (2008–2019), at least 10 years' worth of valid data (Section S2.1). To robustly detect and estimate the trends, we used the non-parametric Mann–Kendall test, along with the Theil–Sen statistical estimator (hereafter, MK–TS) (Theil 1992; Sen 1968). To this end, we used the R package Openair (Carslaw and Ropkins 2012; R Core Team 2021) to obtain the regression parameters for the trends (slope, uncertainty, and *p*-value), estimated via bootstrap resampling, and considered them to be statistically significant if $p < 0.05$.

Based on the data availability constraints, we used data from 414 and 319 AQMSs for the present-day and trend assessments, respectively (see detailed information in Figure S1.2 and Tables S1.1 and S1.2).

Remote sensing

To characterize the spatiotemporal variability of the tropospheric NO_2 (used as a proxy for NOx emissions, Liu et al. 2016) and HCHO (used as a proxy for the total VOC reactivity, Martin et al. 2004), we employed spaceborne observations provided by NASA's ozone monitoring instrument (OMI) aboard the Aura satellite (OMI Team 2012). The OMI follows a sun-synchronous orbit, with a daily overpass at approximately 13:45 h local solar time, and has a resolution of 13×24 km^2. The area assessed included the entire Iberian Peninsula, southern France, and northern Africa. We used official NO_2 and HCHO monthly data obtained from the Quality Assurance for Essential Climate Variables website (QA4ECV) (http://www.qa4ecv.eu, refer to Section S2.2), which was developed within the framework of the EU FP7 project (Boersma et al. 2017; De Smedt et al. 2018). Data is stored in uniform global grids with a $0.25° \times 0.25°$ spatial resolution.

With these monthly data, we calculated April–September averages of tropospheric NO_2, HCHO and the HCHO/NO_2 tropospheric column ratio, used sometimes as an indicator of the O_3 sensitivity regime (Li et al. 2021), for every year for each pixel. Then, we calculated the present-day spatial distribution and estimated the trends.

Emissions of O_3 precursors

We used data on national emissions of relevant O_3 precursors: (i) NOx, VOCs (non-CH_4), and CO contained in the EU emissions inventory report 1990–2020 (EEA 2022) under the UNECE Convention on Long-range Transboundary Air Pollution; and (ii) for CH_4, from the national greenhouse gas inventories submissions to the UNFCCC and the EU Greenhouse Gas Monitoring Mechanism (EU Member States). More information can be found in Section S2.3.

We estimated the trends in the emissions using the Openair MK–TS for 2008–2019. Firstly, we evaluated the Spanish emissions in a European context and, secondly, at a national level with data disaggregated by main emissions sector (using the EEA sector classification; see EEA 2022).

Meteorological parameters

To complement the analysis with other potential factors that might have had an effect on the surface O_3 trends, we used the fifth generation of the European Centre for Medium Range Weather Forecasts (ECMWF) global reanalysis (ERA5). We evaluated monthly averaged meteorological data from the ERA5 reanalysis dataset, which provides a continuous dataset in time and space with a regular $0.25° \times 0.25°$ grid (Hersbach et al. 2019). We selected nine meteorological parameters that might have impacted surface O_3 (Jacob and Winner 2009; von Schneidemesser et al. 2015; Coates et al. 2016; Otero et al. 2016; Lefohn et al. 2018; Wei et al. 2022). These include temperature, downward surface solar radiation, downward UV radiation at the surface, cloud cover, boundary layer height, evaporation, surface wind speed, surface pressure, and total precipitation. Refer to Section S2.4 for information on calculations.

For each grid pixel, we calculated the annual April–September averages in order to determine the present-day (2015–2019) spatial variation, and to estimate the 2008–2019 trends. The trends and level of significance were obtained by adapting the script to calculate the trends for the raster images from Abdi et al. (2019) to be used with the Openair MK–TS. It should be noted that a 12-year dataset

is presumably of limited duration for the detection of climatological trends because, traditionally, at least 30 years' worth of records are needed to identify a genuine trend in climate. Nevertheless, we considered that the statistically significant changes detected, even within this relatively short timeframe, could provide valuable supplementary insights.

Results and discussion

Meteorological parameters

Section S3 presents the results of the analyses concerning meteorological parameters that could have influenced O_3 concentrations during the warm season. Most of the variations observed within the national territory for the period 2008–2019 did not exhibit statistical significance (Figure S3.1), probably due to the relatively short duration of the dataset when viewed from a meteorological/climatological standpoint. Thus, we cannot disregard the importance of exploring other potentially significant trends that could involve examining additional meteorological parameters, employing different and/or less strict statistical approaches, considering alternative temporal aggregations, or extending the analysis over longer timeframes.

Firstly, we briefly discuss the (non-statistically significant) variations in meteorological parameters (see central panels in Fig. 2 and Figure S3.1). A temperature increase was observed practically all over the country (Fig. 2b), consistent with the findings of Borge et al. (2019) for 1993–2017. Moreover, there was a general increase in solar radiation (Figure S3.1b and e), in line with Pfeifroth et al. (2018), and with greater intensity in areas of the south-west, the Mediterranean coast, and northern parts of the country, in logical consonance with the decrease in cloud cover observed over these areas (Figure S3.1 h).

The thickness of the planetary boundary layer (PBL) increased, especially in the interior of the country (Figure S3.1 k), which may have had an effect on the amount of stratospheric and free tropospheric O_3 influencing the ground-level O_3 concentrations. An increase in evaporation was also observed over much of the interior (Figure S3.1q), especially in Castilla-La Mancha and eastern Andalucia. Precipitation showed a decrease throughout the country, in agreement with Borge et al. (2019) for 1993–2017, except in dispersed areas of the north and north-east and inland (Figure S3.1w). The surface wind showed no clear spatial patterns, with regions of the Mediterranean Sea exhibiting decreases, but with no variation, or with slight increases, in inland areas (Figure S3.1n). Azorin-Molina et al. (2016) found wind speed decreases for 1961–2011 in Spain, in line with Garrido-Perez et al. (2018, 2019), that indicated that stagnation, which is an important O_3 driver, increased in Southern Europe in 1998–2015.

Most of the observed variations in the meteorological parameters for the interior and central areas may have been favorable for O_3 production (Jacob and Winner 2009; von Schneidemesser et al. 2015; Otero et al. 2016; Coates et al. 2016; Lefohn et al. 2018; Wei et al. 2022). This may be consistent with the general increase in O_3 concentrations in central Spain found in Massagué et al. (2023). The extent to which such non-statistically significant variations (or others) could have influenced the O_3 concentrations during the study period requires further analysis.

Although the overall temperature increase across the country was not statistically significant, it should be noted that this parameter exhibited a statistically significant increase in most parts of the Madrid region, as well as in some large areas of western CastillaLa Mancha and other dispersed regions (Fig. 2c). This is consistent with the results of Borge et al. (2019) who reported a temperature increase across the country (1993–2017) during the warm season, with the central regions experiencing the greatest rate of increase.

Temperature is the meteorological parameter with the greatest potential impact on ground-level O_3, as supported by studies conducted by Jacob and Winner (2009), Pusede et al. (2015), and Wei et al. (2022). Thus, ground-level O_3

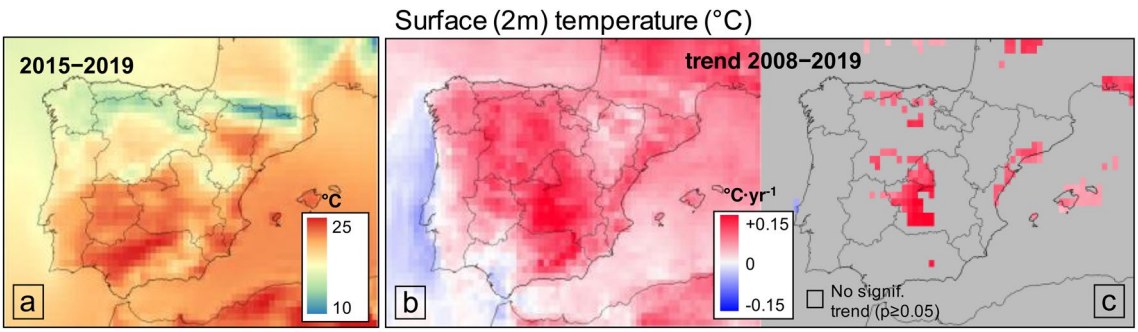

Fig. 2 April–September surface temperatures at 2 m altitude. **a** Present-day (2015–2019); **b** variation (2008–2019); and **c** statistically significant trends (calculated from ERA5 monthly averaged data). See Section S3 for the rest of the meteorological parameters

is strongly correlated with surface temperature, particularly in highly polluted areas (Porter and Heald 2019). Increasing temperatures can enhance O_3 concentrations by accelerating chemical reactions, thereby increasing emissions of biogenic VOCs (BVOCs) (Sillman and Samson 1995; Coates et al. 2016) or through other mechanisms (see Porter and Heald 2019 and reference therein). It should also be considered that, although anthropogenic VOCs (AVOCs) are usually not temperature dependent, evaporative emissions of certain AVOCs can increase with rising temperatures (Rubin et al. 2006). Furthermore, Borge et al. (2019) also determined that weather changes consistent with our findings, including temperature increase, caused increments in O_3 (and other pollutants) in Spain.

O_3 precursors

Present-day O_3 precursors

The present-day distribution of ground-level NO and NO_2 in April–September is shown in Figure S1.3. As expected, the highest concentrations were found in high-traffic environments, especially in large metropolitan areas, such as Barcelona and Madrid, and, to a lesser extent, in northern industrial locations. The lowest concentrations were found in rural, and especially regional, background sites (Figure S1.3a, b, e, and f). Although these concentrations were evaluated during April–September—naturally lower than during colder months—the NO_2 concentrations at many stations were still above the annual NO_2 limit of both the Directive (40 $\mu g \cdot m^{-3}$) (EC 2008) and, obviously, the latest, stricter annual WHO Guideline (10 $\mu g \cdot m^{-3}$) (WHO 2021), with 65% of the AQMSs recording exceedances of this.

The present-day NO_2 tropospheric column spatial distribution (OMI data), often used as a proxy for NOx emissions (Liu et al. 2016), is shown in Fig. 3a. The highest concentrations were recorded in large urban areas, such as Madrid, followed by Barcelona (up to approximately 4×10^{15} molecules$\cdot cm^{-2}$), and, with levels below half, Valencia–Castellón and Sevilla. Significant tropospheric NO_2 levels were also recorded in the Gibraltar Strait and the Alborán Sea, probably caused by heavy maritime traffic (Nunes et al. 2020), a large maritime area in the south of Marseille, and in the northern industrial areas of Oviedo–Gijón, Coruña, and Bilbao.

To partly overcome the lack of detailed in situ VOC measurements, we here briefly discuss the variability in the HCHO tropospheric columns obtained from the OMI (Fig. 3d). HCHO is a frequent by-product of the oxidation of VOCs, and is thus sometimes used as a proxy for the total VOC reactivity (Martin et al. 2004). A common issue of current space-based HCHO observations lies in their relatively weak signal-to-noise ratio, which greatly limits their interpretation, except in regions of the world with strong HCHO levels (e.g., the tropics, eastern USA, and Asia). However, when focusing on April–September (the seasonal maximum for HCHO), some spatial variability can still be observed over the Iberian Peninsula, with tropospheric columns ranging between 5 and 10×10^{15} molecules$\cdot cm^{-2}$. The lowest values were observed over the central Pyrenees and in specific rural areas, whereas highest values occurred predominantly over northeastern Spain and Portugal. The highest HCHO in the northeast was probably a combination of high isoprene emissions and the transport of aged high-O_3 air masses from the coast. Overall, no clear HCHO hotspots were observed over the main Spanish urban areas, which suggests a predominantly biogenic origin (including, for instance, the oxidation of biogenic isoprene), although some smaller and/or weaker hotspots could be hidden by the aforementioned signal-to-noise ratio (and the still-coarse spatial resolution of the OMI observations).

Given the weaker spatial variability of HCHO compared to NO_2, the HCHO/NO_2 tropospheric column ratio tended to follow a similar spatial distribution as 1/NO_2 tropospheric columns (Fig. 3g). Although this ratio is sometimes used as an indicator of the O_3 sensitivity regime (NOx-limited versus VOC-limited) (Li et al. 2021), the threshold distinguishing both regimes can vary substantially in time and space, and undefined regimes can prevail over a rather large range of HCHO/NO_2 values, which limits its interpretability (Souri et al. 2020, 2022). Nonetheless, the present-day mean April–September HCHO/NO_2 values ranged between 2 and 11, suggesting a predominantly NOx-limited regime over Spain, with NOx most strongly limited over the Spain–Portugal and Spain–France (Pyrenees) border regions. Lower values of this ratio were logically found over large NO_2 hotspots. It is worth noting that these results were obtained in the early afternoon (the OMI overpass being at around 13:45 h local solar time), thus not during the morning rush hours when BVOC emissions tend to be lower and NOx emissions higher, and thereby causing the HCHO/NO_2 values to significantly change.

Trends of O_3 precursors

The assessment of ground-level NO and NO_2 (April–September) trends is shown in Figure S1.3. The results showed that a relevant proportion (39%) of the AQMSs recorded downward NO trends across the country in 2008–2019 (Figure S1.3c), with the largest absolute decreases mostly occurring in northern locations and a few specific sites in Barcelona, especially in the urban and high-traffic environments (Figure S1.3d). In the Madrid area and in eastern and southern areas (including Sevilla and Valencia), the absolute average NO decreases were weak. However, a detailed comparison between Madrid and Barcelona (Table S1.3)

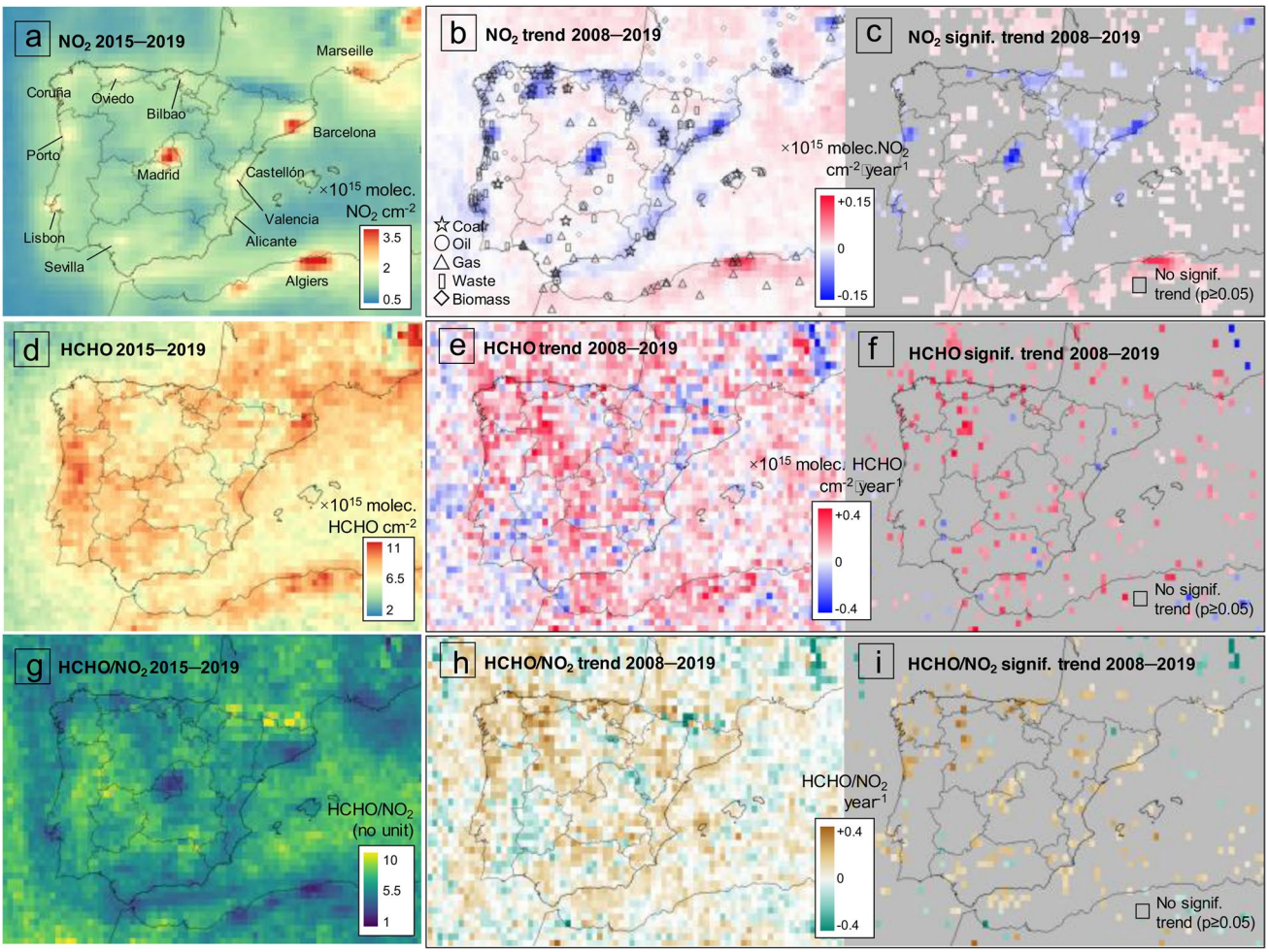

Fig. 3 Spatial distribution of NO_2 and HCHO tropospheric columns for April–September measured by OMI-NASA and HCHO/NO_2 ratio. Each pixel covers an area of 13 × 24 km^2. **a**, **d**, **g** Present-day (2015–2019) spatial variability; **b, e**, **h** absolute trends for 2008–2019; and **c**, **f**, **i** absolute trends for 2008–2019, showing only pixels with statistically significant ($p < 0.05$) trends. Gray pixels—$p \geq 0.05$. Relative variations (in %) can be found in Figure S1.4 in the Supplemental Information. Map 3b shows the locations of the power plants operational in 2018 (from Byers et al. 2021)

showed that, on average, the NO absolute decreases were similar (-0.5 μg·m^{-3}·$year^{-1}$), although, in relative terms, the NO decreases were more intense in Madrid (-5.0%·$year^{-1}$) than in Barcelona (-3.5%·$year^{-1}$), considering all types of AQMSs, and also only traffic. Similarly to the NO, 40% of the stations recorded downward NO_2 trends (Figure S1.3 g), most of them located in the northern half of the country. The largest absolute decreases were also mostly recorded in the northern areas, including Barcelona. In Madrid, a large proportion of AQMSs did not record significant trends. Again, in absolute terms, the average decreases were similar in Madrid and Barcelona (-0.8 μg·m^{-3}·$year^{-1}$) (Table S1.3), although in relative terms, the NO_2 decreases were more intense in Madrid (-3.0%·$year^{-1}$) than in Barcelona (-2.4%·$year^{-1}$). Throughout the Mediterranean coastal area (except in Catalonia), practically no NO_2 downward trends were recorded. In Sevilla and along the Guadalquivir Valley, several AQMSs recorded NO_2 downward trends, but these were of very low intensity. As for NO, the strongest NO_2 decreases were mainly driven by changes in traffic (either quantity or type), as these were observed especially at traffic stations (Figure S1.3 h and Table S1.3).

Figure 3b shows the variation in the April–September tropospheric NO_2 for 2008–2019, while Fig. 3c provides an estimation of the statistically significant trends ($p < 0.05$) (see Figure S1.4 for relative variations). The Oviedo–Gijón and León areas in northwestern Spain have been historically highly industrialized, with the highest density of coal-powered plants in the country (indicated in Fig. 3b). These plants were associated with high tropospheric NO_2 levels (Cuevas et al. 2014). In the last decade, many of these plants have reduced/stopped their operations or have applied

measures to reduce their atmospheric emissions (e.g., Directive 2010/75/EU) (REE 2021), potentially contributing to two outcomes: firstly, the clear decrease as shown in Fig. 3b in the northwest (similar to findings by Castellanos and Boersma 2012), probably statistically insignificant because of sudden changes in NOx emissions (e.g., from the closure of large power plants). Secondly, the explanation for why these areas do not appear as NO_2 hotspots in the present-day (2015–2019) (Fig. 3a). Additionally, decreases in the NO_2 tropospheric columns were recorded in highly industrialized and/or high-traffic areas, such as Barcelona–Tarragona, the entire Ebro Valley, País Vasco–Santander, and the eastern coastal strip, likely as a result of implemented control measures. According to the European Environmental Agency's Emission Inventory Report (EEA 2022), NOx declining emissions in Spain were driven by three key sectors: (i) the energy sector through the adoption of renewable energy, abatement techniques in thermal power plants, and transitioning to combined cycle gas plants; (ii) road transport, due to Euro standards implementations; and (iii) the industry sector, driven by abatement techniques and a shift to natural gas, particularly in non-metallic minerals. For detailed information on NOx and other O_3 precursor emissions in Spain, see MITERD (2023), and refer to Section S4 for relevant emissions abatement policies.

Most of the downward tropospheric NO_2 trends were statistically significant. The most marked declines were mainly found in/around Madrid, both in absolute (Fig. 3c) and relative (Figure S1.4 a, b) terms. To a lesser extent, similar declines were observed in/around Barcelona, with a maximum absolute decreasing rate approximately 30% lower than that in Madrid. This pattern was followed by industrial/urban areas like Oviedo, País Vasco and Cantabria, and part of the Ebro Valley (that includes a major coal-fired plant), with maximum absolute decreasing rates roughly 60% lower than in Madrid. Statistically significant downward trends on tropospheric NO_2 were also detected in Sevilla and Puertollano, in this latter area despite the reduced area of the closed basin and the relatively coarse spatial resolution of OMI. It is relevant that, in Barcelona city, the decreases found were weaker than in other areas with similar present-day levels of tropospheric NO_2, such as Madrid (Fig. 3a).

At first glance, the variations in satellite-based and ground-level NO_2 show similarities. For example, in qualitative terms, the tropospheric NO_2 decreases in large areas of the north, the Ebro Valley, and the large urban areas of Madrid and Barcelona are consistent with those from the ground-level measurements. However, over large parts of the Mediterranean coast, where tropospheric column NO_2 levels also clearly declined (Figs. 3c, S1.4b), the AQMSs mostly did not detect any NO_2 trends (Figure S1.3 g). The measurements obtained using these different tools are not directly comparable here, but are complementary (Bechle et al. 2013), since their spatial and temporal representativeness are different. For instance, ground-based observations provide concentrations at specific locations that can be highly influenced by nearby sources, whereas satellite-based observations measure average concentrations integrated over specific land areas (several square kilometers) and in the vertical. Similarly, satellite-based observations have a daily frequency, typically in the afternoon (subject to cloud cover limitations and associated biases), while ground-based observations are daily averages derived from 24-h data. In any case, to support the interpretation of O_3 trends, a wider representation of the NO_2 load in a large air mass is desirable.

Over the same period, the statistically significant trends affecting the HCHO tropospheric columns were mostly positive, albeit scarce and dispersed over the peninsula, with no clear spatial patterns discernable (Fig. 3f). The aforementioned noise affecting these measurements added uncertainties, making it difficult to detect significant trends over the relatively short time period of 12 years. The highest positive HCHO trends were observed in northwestern Spain. Similarly, the significant HCHO/NO_2 ratio trends were dispersed and mostly positive (Fig. 3i). In large cities like Madrid or Barcelona, this increase might have been partially driven by the reduction in NO_2, whereas in northwestern Spain, it is likely to have been driven by the increase in HCHO. Overall, under the assumption that HCHO tropospheric columns are a reliable proxy for total VOC reactivity, these results suggest that, at least in the early afternoon when the OMI observations are available, NOx tends to play an increasingly important, albeit perhaps not entirely limiting, role in the formation of O_3 over Iberia.

The mostly increasing HCHO trends are qualitatively consistent with those of Opacka et al. (2021), who found positive isoprene and HCHO trends over Iberia (2001–2016), attributing them to changes in the land cover. However, as background O_3 concentrations have increased (Sicard 2021), and HCHO can be generated from VOCs (including isoprene) (Wolfe et al. 2016) by O_3 oxidation, it is plausible that this global O_3 increase contributed to the HCHO increase.

Trends in emissions of the main O_3 precursors

Although inventories only consider emissions of anthropogenic origin, it should be noted that biogenic emissions of precursors can have a large impact on O_3 (Monks et al. 2015). For instance, among the most important O_3 precursors, and at a global scale, 90% of atmospheric VOCs are biogenic, isoprene, and monoterpenes being the greatest contributors (Guenther et al. 1995), or 15% of global NOx emissions originate from soils, which can be a significant

source of the NOx budget outside the cities (Weng et al. 2020). However, at local/regional scales, these contributions can change dramatically (Sartelet et al. 2012), for instance, in situations where O_3 pollution episodes occurr in Spain, mostly in and around highly populated and/or industrialized conurbations (Querol et al. 2016).

The inventories showed that, in 2008–2019, emissions of the main anthropogenic precursors of O_3 evolved differently in the EU-28 and Spain (Fig. 4a, b). In the EU-28, all compounds declined (-1.3 to $-2.9\%\cdot year^{-1}$). However in Spain, NOx steadily declined ($-3.4\%\cdot year^{-1}$), but AVOCs, CO, and CH_4 increased from 2014, probably indicating a rebound of emissions after the financial crisis (Pacca et al. 2020), although they slightly declined overall in 2008–2019, following no statistically significant trends (only $p<0.1$ for CH_4). The AVOC/NOx ratio in Spain significantly increased

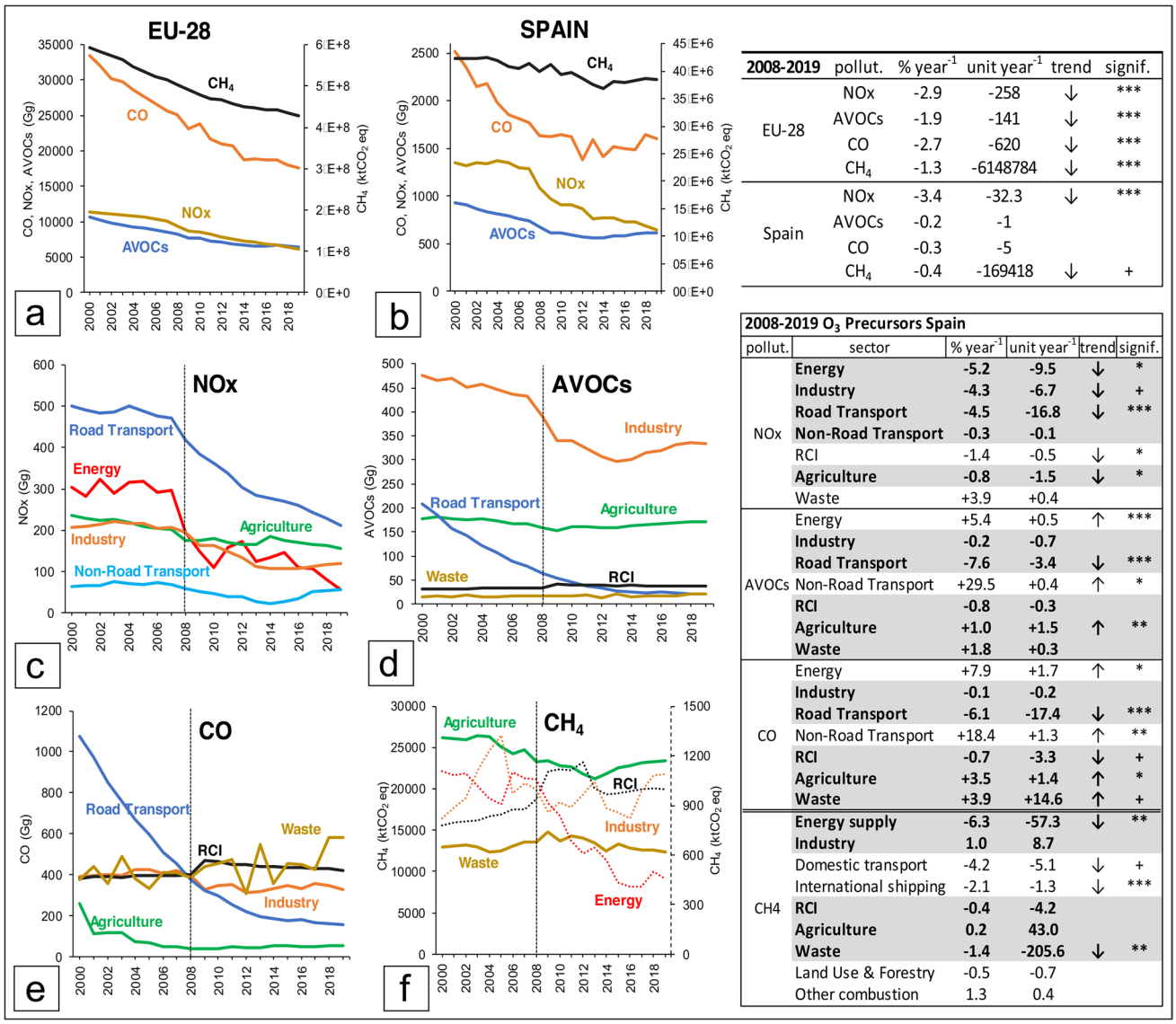

2008-2019	pollut.	% year^{-1}	unit year^{-1}	trend	signif.
EU-28	NOx	-2.9	-258	↓	***
	AVOCs	-1.9	-141	↓	***
	CO	-2.7	-620	↓	***
	CH_4	-1.3	-6148784	↓	***
Spain	NOx	-3.4	-32.3	↓	***
	AVOCs	-0.2	-1		
	CO	-0.3	-5		
	CH_4	-0.4	-169418	↓	+

2008-2019 O_3 Precursors Spain					
pollut.	sector	% year^{-1}	unit year^{-1}	trend	signif.
NOx	**Energy**	**-5.2**	**-9.5**	↓	*
	Industry	**-4.3**	**-6.7**	↓	+
	Road Transport	**-4.5**	**-16.8**	↓	***
	Non-Road Transport	**-0.3**	**-0.1**		
	RCI	-1.4	-0.5	↓	*
	Agriculture	**-0.8**	**-1.5**	↓	*
	Waste	+3.9	+0.4		
AVOCs	Energy	+5.4	+0.5	↑	***
	Industry	**-0.2**	**-0.7**		
	Road Transport	**-7.6**	**-3.4**	↓	***
	Non-Road Transport	+29.5	+0.4	↑	*
	RCI	**-0.8**	**-0.3**		
	Agriculture	**+1.0**	**+1.5**	↑	**
	Waste	**+1.8**	**+0.3**		
CO	Energy	+7.9	+1.7	↑	*
	Industry	**-0.1**	**-0.2**		
	Road Transport	**-6.1**	**-17.4**	↓	***
	Non-Road Transport	+18.4	+1.3	↑	**
	RCI	**-0.7**	**-3.3**	↓	+
	Agriculture	**+3.5**	**+1.4**	↑	*
	Waste	**+3.9**	**+14.6**	↑	+
CH4	**Energy supply**	**-6.3**	**-57.3**	↓	**
	Industry	**1.0**	**8.7**		
	Domestic transport	-4.2	-5.1	↓	+
	International shipping	-2.1	-1.3	↓	***
	RCI	**-0.4**	**-4.2**		
	Agriculture	**0.2**	**43.0**		
	Waste	**-1.4**	**-205.6**	↓	**
	Land Use & Forestry	-0.5	-0.7		
	Other combustion	1.3	0.4		

Fig. 4 **a**, **b** Emissions of the main O_3 precursors (NOx, AVOCs, and CO in Gg, CH_4 in $ktCO_2$ eq.) from the EU-28 and Spain, 2000–2019. In the top right table, estimation of 2008–2019 trends by region and compound. Trend magnitudes are significant at $p<0.001$ (***), $p<0.01$ (**), $p<0.05$ (*), and $p<0.1$ (+); blank—no statistical significance ($p\geq0.1$). **c**–**f** Emissions of the main O_3 precursors by sector in Spain for 2000–2019. Only the top five sectors are shown. RCI—residential/commercial/institutional. **f** For CH_4, the sectors have a different classification because they came from a different database (EEA 2021c). Note that the secondary (right) *y*-axis shows the emissions sectors (dotted lines—industry, residential, and energy supply) plotted one order of magnitude below agriculture and waste on the primary *y*-axis. In the bottom right table, estimation of 2008–2019 trends by compound and sector in Spain. Only the top five sectors are plotted in the charts. In the table, these are highlighted in gray and in bold, while the others are retained for reference. NOx, AVOCs, and CO data from EEA (2021b)

during this period, by 1.6 times from 2007 to 2019, which is in general agreement with the trends observed for the $HCHO/NO_2$ ratio (Fig. 3i). A breakdown of the variations in emissions by region is unavailable at present, but information on the emissions sectors at the national level is accessible (Fig. 4c–f).

In 2008–2019, three of the top five NOx-emitting sectors in Spain (industry, energy, and road transport) significantly decreased their NOx emissions (-4.3 to $-5.2\%{\cdot}year^{-1}$). Emissions from agriculture slightly decreased ($-0.8\%{\cdot}year^{-1}$), and those from non-road transport showed no significant trend, albeit they increased from 2014 (Fig. 4c).

The most relevant AVOCs-emitting sectors are industry (including emissions from solvents), followed by agriculture (representing less than half the industrial emissions), and residential/commercial/institutional (RCI), road transport, and waste, all representing less than 15% of the industrial emissions. The AVOCs emissions from the industrial sector did not follow a trend, although, after 2013, they clearly increased. Agricultural emissions weakly increased ($+1.0\%{\cdot}year^{-1}$) along the period, while RCI and waste AVOCs emissions did not follow any trends. Finally, road transport emissions of AVOCs strongly decreased ($-7.6\%{\cdot}year^{-1}$) (Fig. 4d).

The top five CO-emitting sectors are waste, then RCI, industry, road transport, and agriculture. Road transport CO strongly decreased ($-6.1\%{\cdot}year^{-1}$) and RCI emissions also decreased, but only slightly ($-0.7\%{\cdot}year^{-1}$). Conversely, the CO from industry did not change during the studied period, whereas that from the agricultural and waste sectors clearly increased ($+3.5$ and $+3.9\%{\cdot}year^{-1}$, respectively) (Fig. 4e).

The most relevant CH_4-emitting sector is agriculture, followed by waste management, then, more than an order of magnitude below, by industry, RCI, and energy. The agricultural sector showed no trend for 2008–2019, but did steadily increase from 2013, whereas waste management (representing about half the agricultural sector emissions) decreased by $-1.4\%{\cdot}year^{-1}$ (Fig. 4f).

Interpretation of O_3 trends in specific areas

Massagué et al. (2023) found statistically significant O_3 trends in the Spanish O_3 hotspots for 2008–2019. However, these trends were observed in only a relatively small proportion of the AQMSs, in line with the findings of other studies in which similar time periods were analyzed (Fleming et al. 2018; Mills et al. 2018; EEA 2020). This is partly attributed to the meteorological sensitivity of O_3, which varies from year to year, thereby complicating the detection of trends on relatively short timescales (Colette et al. 2016; Fleming et al. 2018). Moreover, depending on the part of the O_3 distribution under consideration, an individual time series may show opposite trends, potentially leading to differing conclusions in the evaluation of emissions control strategies (Lefohn et al. 2017, 2018; Yan et al. 2019). For this reason, Massagué et al. (2023) employed a variety of metrics associated with different O_3 concentration levels. Moderate O_3 concentrations were evaluated using the annual mean O_3 concentrations (O3YR), while mid to high O_3 concentrations, by means of the well-established SOMO35, AOT40, and 93.2 percentile (P93.2) of the maximum daily 8-h average (MDA8). Furthermore, peak O_3 concentrations were evaluated using the fourth highest MDA8 within a year (4MDA8) and the number of exceedances of Europe's hourly information threshold (IT) ($180\ \mu g{\cdot}m^{-3}$). This approach allowed for the assessment of a wide range of the distribution of O_3 concentrations.

The main hotspots followed contrasting O_3 trends (Fig. 1b). The Madrid area had mostly upward O_3 trends for all the metrics and, in many cases, the highest increasing rates. The interior of the Valencian Community had a mixed variation pattern, depending on the specific O_3 metric considered. The area north (downwind) of Barcelona, the Puertollano Basin, and the Guadalquivir Valley revealed almost no variations, and Sevilla was the only major Spanish city where O_3 mostly decreased and, in many cases, with the highest decreasing rates. Multiple causes might explain these contrasting O_3 trend behaviors in Spain, some of which are discussed below.

Increasing O_3 trends in the Madrid area

This O_3 hotspot (Fig. 1a), located on a continental plateau (700 m a.s.l.), is frequently affected by high O_3 episodes caused by intense NO_2 emissions, mainly from traffic coupled with high BVOCs. During the typical summer anticyclonic conditions, the surrounding mountain ranges enhance stagnant conditions and trigger recirculations, which lead to acute O_3 episodes (see Querol et al. 2016 and references therein).

As previously mentioned, the Madrid area experienced a statistically significant upward trend in temperature during the study period, which might have enhanced the O_3 levels, albeit to a limited extent, through various mechanisms (Porter and Heald 2019 and references therein). These mechanisms include an increase in BVOC emissions (Sillman and Samson 1995) and, to a minor degree, emissions from specific AVOCs (Rubin et al. 2006). The variations in other meteorological parameters observed in the interior areas, which can be conducive to O_3 production, such as increasing solar radiation, an increase in PBL thickness, and a decrease in cloud cover, although lacking statistical significance, might still have contributed to the observed increase in O_3 levels (see the "Meteorological parameters" section). Furthermore, as depicted in Figure S3.1j, the Madrid area typically reaches high PBL thicknesses due to the intensive convective circulations that give rise to the usual Iberian thermal low (Millán et al. 1997, 2002). These high convective flows may account for a greater influence of stratospheric and free

tropospheric O_3 (which is globally increasing, depending on the location) (Monks et al. 2015) via mixing down to the surface and impacting ground-level concentrations.

In terms of emissions of O_3 precursors, the road transport sector in Madrid stands as the largest contributor to the share of NOx emissions (Borge et al. 2014). Additionally, it contributes significantly more to NOx emissions in Madrid than in Barcelona (Valverde et al. 2016), where other sectors account for significantly higher proportions (Guevara et al. 2014; Soret et al. 2014) (see Figure S1.5a). Assuming that the national 50% reduction in NOx emissions from road transport (Fig. 4c) applies similarly to both metropolitan areas for 2008–2019 (or potentially even higher in Madrid, as suggested by the ground-level measurements, Table S1.3), this would explain the substantial decrease in tropospheric NO_2 observed by the OMI over the Madrid area, while Barcelona experienced a less pronounced decline. Because local O_3 production depends on the VOC/NOx ratio, in urban or industrialized areas with high NOx concentrations, such as Madrid (and Barcelona), the VOC/NOx ratio is low, and O_3 formation tends to be VOC-limited (Sillman et al. 2003), as also suggested by the lowest national HCHO/NO_2 ratios reported in Fig. 3, especially for the Madrid area. Under these (VOC-limited) conditions, a reduction in NOx emissions might cause an increase in O_3 (Monks et al. 2015). In this context, the marked NOx decreases over Madrid, as observed by the OMI and mainly related to road transport, partially might explain the generalized upward trends in O_3 in this area for 2008–2019. Additionally, as Saiz-Lopez et al. (2017) also proposed for the same area during 2007–2014, it is likely that a portion of the observed increasing O_3 trends, particularly in the case of moderate O_3 metrics like O3YR or SOMO35 (Lefohn et al. 2017; Fleming et al. 2018), can be attributed to a reduction in the NO titration effect (Sicard et al. 2013, 2016; Simon et al. 2015). This is supported by the fact that these O_3 trends were detected in urban and/or traffic stations, which also recorded large NO decreases (as documented in Table S1.3).

The clear increase in industrial AVOC emissions since 2013, with this sector being the largest contributor to AVOC emissions in Spain (Fig. 4) and bearing the dominant responsibility for the largest share of AVOC emissions in Madrid (Figure S1.5b), coupled with significant increases in emissions from other sectors, may also have contributed to the general upward trend in O_3 levels in the Madrid area. Increases in VOC emissions, which are known to cause increases in O_3 under VOC-limited conditions, may have been particularly influential in this regard, according to previous research (Jacob et al. 1995; Sillman 1999; Sillman and He 2002; Sillman et al. 2003).

Finally, it is worth mentioning the case of two AQMSs located in Castilla La Mancha, 40 km north-east of central Madrid, in an area likely prone to be in NOx-limited conditions. These stations, which are affected by the pollution plume from the Madrid area and typically experience high levels of O_3, recorded statistically significant decreasing trends for certain O_3 metrics, contrasting with the generalized increasing trends observed nearer to the urban area (Massagué et al. 2023). This situation illustrates how NOx reductions can impact O_3 trends, depending on different O_3 formation regimes.

Absence of O_3 trends in the northern Barcelona area

The Vic Plain (located downwind of Barcelona) (Fig. 1a) is an important O_3 hotspot in Spain, partly due to the high precursor emissions transported from the Barcelona metropolitan area (Diéguez et al. 2009; Querol et al. 2016, 2017). This region is affected by the large-scale WMB recirculations (see Querol et al. 2016 and references therein). Its proximity to the sea causes a thinner PBL in this area compared to the interior areas, such as the Madrid region (Figure S3.1 k), which likely means Barcelona is less affected by air masses from the free troposphere.

Massagué et al. (2023) found no statistically significant O_3 trends in this hotspot, thus the intense reduction in NOx emissions in the Barcelona area, as evidenced by both satellite-based (Fig. 3c) and ground-level (Figure S1.3) measurements, likely had a limited or no impact on the O_3 levels at this location. The decrease in tropospheric NO_2 in the Barcelona area was less intense than in Madrid, probably because NOx emissions from sectors other than road transport (industry, harbor, energy, among others), which contribute more to the NOx share in Barcelona than in Madrid (Guevara et al. 2014; Soret et al. 2014), decreased less than those from road transport, or even increased (Fig. 4c).

The absence of significant meteorological variations likely also contributed to the lack of change in O_3 levels in this area, in contrast to central Spain and, therefore, the Madrid area. However, a few rural background sites not located in the Vic Plain, but also affected by the Barcelona area's pollution plume, recorded slight downward trends for the high and peak O_3 metrics (P93.2 and 4MDA8), consistent with the findings of Lefohn et al. (2018) and Yan et al. (2019) who indicated that, at most stations in Europe, O_3 in the upper end of the distribution decreased due to effective NOx abatement measures.

In Barcelona city, only some urban traffic sites recorded increasing trends for several O_3 metrics in 2008–2019 (Massagué et al. 2023), pointing to the effect of lower titration by NO (Simon et al. 2015; Sicard et al. 2013, 2016), which is supported by the marked ground-level NO decreases recorded during that period at those same sites (Figure S1.3).

Mixed O_3 trends in the Valencian Community

The O_3 phenomenology in the Valencian Community (Fig. 1a) resembles that of Barcelona–Vic Plain because this region lies in the WMB and is also affected by large-scale recirculations, where O_3 episodes occur inland due

to high urban (Alicante and Valencia) and urban-industrial (Castellón) emissions that are transported inland by mesometeorological circulations (e.g., Millán et al. 1997, 2000).

According to Massagué et al. (2023), the Valencian Community was the O_3 hotspot with the second highest number of positive trends after Madrid. Trends in the metrics based on moderate and mid to high concentrations were mostly positive, found in coastal locations, and, to a lesser extent, in the interior. In addition, a few rural and regional AQMSs recorded downward trends for peak O_3 in the north-west.

Levels of tropospheric column NO_2 decreased only in Valencia and Alicante (Fig. 3c), where road transport prevails as a main NOx source. However, no statistically significant trends were found for Castellón, where high industrial emissions, mainly from the ceramics cluster, a petrochemical plant, and a power plant (Minguillón et al. 2013), likely moderated the NOx reductions from road transport. Although there is no data available on the share of O_3 precursor emissions in the Valencian Community, it is known that the industrial and agricultural economic sectors are (relatively) more important there than in Madrid (INE 2022). Therefore, the relative weight of the emissions from these (and other) sectors might have been expected to be greater in the Valencian Community, and these emissions showed minor decreases, stability or even increases in the period studied (Fig. 4c, d, e).

The absence of evident variations in meteorological parameters may indicate that the dominant increasing O_3 trends in the region (mostly occurring in the coastal cities) are probably due to the decrease in NOx emissions in a VOC-limited regime and/or by a lower NO titration effect (Simon et al. 2015; Sicard et al. 2013, 2016). However, the decreasing O_3 trends for peak O_3 (4MDA8) in regional background sites located north of the Valencian Community (probably in NOx-limited conditions) might be attributable to the significant reduction in nearby NOx emissions (observed in the tropospheric column) (Figs. 3c and S1.4b). This reduction in NOx emissions, is due to the gradual reduction in the operational activities of one of Spain's largest coal-fired power plants (1050 MW), which formerly had a notable impact on the air quality of this region. The plant's activity began to diminish in 2010 and eventually ceased operations in 2020.

Absence of O_3 trends in Puertollano

In Puertollano, the coexistence of large industrial sources with specific orographic features and atmospheric conditions, such as thermal inversion and stagnation, have resulted in this location having one of the poorest dispersion characteristics among the inland areas of Spain (Diéguez et al. 2009, 2014). The large industrial plant in Puertollano is the main source of NOx and AVOC emissions in the region (Querol et al. 2016 and references therein), and concentrations of hydrocarbons there have been found to be higher than in other large industrial facilities (Diéguez et al. 2009), thus the O_3 formation regime should tend to be NOx-limited. Episodes of O_3 in this closed basin are characterized by their acute nature, where exceedances of Europe's IT are recorded multiple times every year, but only at two closely located AQMSs. However, when considering O_3 metrics indicative of chronic pollution, the AQMSs in Puertollano tend to register lower values than other AQMSs in nearby areas (Massagué et al. 2023).

Satellite observations have shown a slight decrease in NO_2 levels in Puertollano, possibly due to a reduction in industrial NOx emissions (Fig. 3c). However, unlike other cities that experienced a significant reduction in ground-level NOx due to decreased road traffic, Puertollano did not show any decrease (Figure S1.3). This difference may have caused the absence of positive trends in moderate O_3 metrics in Puertollano, as reported in Massagué et al. (2023), which were observed in most cities and are likely due to the effect of reduced NO titration.

According to the inventories, AVOC emissions from the industrial sector did not show a clear trend for the whole period (Fig. 4d), but have clearly increased since 2013–2014, likely due to the rebound effect after the 2008 financial crisis (Pacca et al. 2020). These changes in AVOC emissions may have had a limited effect on O_3 levels in NOx-limited conditions (Sillman 1999; Sillman and He 2002; Sillman et al. 2003).

The temperature changes conducive to O_3 production, together with other non-statistically significant meteorological changes observed in Puertollano in the studied period, are similar to those observed in the Madrid region (Figs. 2c and S3.1). However, it appears that temperature and other meteorological parameters may have a comparatively smaller influence on O_3 levels in the Puertollano area than in other O_3 hotspots because O_3 episodes in Puertollano can occur throughout the year, including winter, rather than being limited to the typical O_3 season (Diéguez et al. 2009).

Decreasing O_3 trends in Sevilla and absence of trends in the Guadalquivir Valley

The urban area of Sevilla, located in the Guadalquivir Valley and downwind of the large petrochemical area of Huelva (Fig. 1a), frequently experiences acute O_3 episodes (Diéguez et al. 2009; Querol et al. 2016), with 1-h concentration-based thresholds being exceeded. However, in inland areas of the Guadalquivir Valley, located downwind of Sevilla and Huelva, O_3 pollution exhibits chronic behavior, where, instead of high hourly threshold exceedances, MDA8 concentration-based thresholds are exceeded for several days during summer (Massagué et al. 2021, 2023).

No AQMSs in this basin recorded any O_3 trends except for in the city of Sevilla, which showed clear and widespread downward trends for most of the O_3 metrics (Massagué et al. 2023). The reason behind the distinctive decreasing O_3 trends in Sevilla city may be attributable to the relatively high urban NOx concentrations that interact with the high AVOC concentrations emitted from the large industrial petrochemical area in Huelva, located upwind (although not evident in Fig. 3d, as no HCHO hotspots were detected). This unique scenario in Spain might have transformed the typical urban VOC-limited regime into one that tends to be NOx-limited (Diéguez et al. 2009). Therefore, changes in the emissions in Sevilla (decrease in NOx, as observed by the OMI) (Fig. 3c) and/or Huelva (which were not observed in this study) may have played a part in causing the overall O_3 decrease in this city.

Importantly, only the low O_3 concentration metrics (in this case annual O_3) increased in this city, which supports the possibility of a reduced NO titration effect (Simon et al. 2015; Sicard et al. 2013, 2016) being the primary cause, similarly to most of the cities studied here, as evidenced by the decrease in ground-level NO concentrations (Figure S1.3c).

The highest national temperatures recorded during the O_3 season were observed along the Guadalquivir Valley (Fig. 2a), which may trigger BVOC emissions from the large forested and planted areas. However, no significant trends in temperature or other evaluated meteorological parameters were found in the analysis. The national inventories showed an increase in agricultural AVOCs, which likely had relevance in Andalucia (and therefore in the Guadalquivir Valley, where most crops are located, as shown in Figure S1.1b), since this sector plays an important role in the local economy (INE 2022). Although increases in HCHO were observed in the Guadalquivir Valley, which would be consistent with the increase in AVOCs from agriculture, these are not clearly distinguishable likely due to the aforementioned signal-to-noise ratio. However, it should be noted that in NOx-limited environments—likely most of the Guadalquivir Valley (also suggested by the HCHO/NO_2 ratio) and also Sevilla (Diéguez et al. 2009)—an increase in VOC emissions has a limited effect on O_3 (Sillman 1999; Sillman and He 2002; Sillman et al. 2003), although it contributes to maintaining the area in a NOx-limited regime.

Other considerations for O_3 trends

Other considerations need to be taken into account when interpreting O_3 trends:

- Concentrations of CH_4 have increased globally in the last decade (Saunois et al. 2020), causing increases in the background O_3 (Archibald et al. 2020) and counterbalancing, to some degree, the decline in European emissions of O_3 precursors (EEA 2020). Thus, non-European sources of CH_4 (and other O_3 precursors) may play a relevant role in ground-level O_3 levels in Europe. However their influence tends to be more pronounced on the annual mean O_3 levels compared to other metrics like SOMO35, which mainly depends on high summer O_3 concentrations and is more influenced by European precursor emissions (Jonson et al. 2018; Turnock et al. 2018; EEA 2020). At a local/regional level, CH_4 emissions also need to be considered because their contribution to regional O_3 formation is nowadays considered to be higher than previously reported (Van Dingenen et al. 2018; IPCC 2021), although in the urban atmosphere, its contribution can be relatively small, where reactive organic compounds and CO dominate O_3 production (Archibald et al. 2020). Despite the lack of data on the relative by-region CH_4 emissions weights in Spain, these might have had an influence on the O_3 trends because, for example, during this period, national emissions from agriculture and waste management (one order of magnitude larger than the other CH_4 emissions sectors considered) increased from 2013, or slightly decreased (Fig. 4f). Furthermore, very high CH_4 emissions have been recently detected seeping from Madrid landfills (ESA 2021; Tu et al. 2022) that have probably been underestimated in the inventories, and these might have had a positive influence on the O_3 levels in and around Madrid, as well as other areas during the period.
- It is possible that other emissions relevant to O_3, such as those from agricultural and biomass burning for power generation (e.g., In 't Veld et al. 2021), might not have been considered or may have been underestimated in the inventories used here. Shipping emissions also need to be considered because they may increase O_3 along the Spanish coastal regions (Jonson et al. 2020; Nunes et al. 2020). For example, emissions in the area between continental Spain and the Balearic Islands—probably relevant to the O_3 in Cataluña and the Valencian Community—might have increased, as port traffic (and other shipping metrics) strongly increased during the study period (Figure S1.6). However, the NO_2 tropospheric columns did not show a clear pattern, with increases recorded in the area around the Balearic Islands, but decreases along the Catalan coast (Fig. 3). In this context, to illustrate the significance of these emissions, the abrupt reductions in shipping traffic, particularly from cruises and ferries, (and air traffic emissions) caused by the COVID-19 restrictions in 2020 and 2021 (Guevara et al. 2022; Puertos del Estado 2022), likely played a role in preventing the European Union's established O_3 thresholds from being exceeded for the first time in the Spanish Mediterranean coastal areas (Querol et al. 2021; Targa et al.

2022). This is because the relatively low reductions in road transport emissions observed in summer, when O_3 levels are at their highest, may not fully account for the large improvement in O_3 levels (Oliveira et al. 2023).

- It is important to acknowledge that other factors operating at different spatial and temporal scales than those considered in this study may also have contributed to the observed trends in O_3. These factors, among others, include the following: (i) the long-range transport of O_3 and its precursors, although the two stations that best represent the regional O_3 behavior in Spain (located on the western Atlantic coast and in the Balearic Islands) (Diéguez et al. 2009) did not capture any O_3 trends during the period (Massagué et al. 2023); (ii) the exchange of O_3 between the stratosphere and troposphere; and (iii) climate variability at both high and low frequencies. For instance, climate phenomena, such as the El Niño–Southern Oscillation or the North Atlantic Oscillation, as well as global warming, can modulate the tropospheric O_3 burden. These factors are interconnected with each other as well as with the other factors considered in this study. To fully understand their impact on surface O_3 trends, complex modeling tools are necessary.

Conclusions

A related study (Massagué et al. 2023) revealed contrasting surface ozone (O_3) trends among the O_3 hotspots in Spain from 2008 to 2019. Specifically: (i) the Madrid metropolitan area showed generalized upward trends, often with the highest increasing rates; (ii) the interior of the Valencian Community area had a mixed variation pattern; (iii) the area downwind of Barcelona, the Puertollano Basin, and the Guadalquivir Valley showed no variations; and (iv) Sevilla was the only major urban area in Spain that recorded general decreasing trends.

While understanding the drivers behind these contrasting O_3 trends requires the use of highly complex models, this study aimed to make progress toward this goal by employing a simplified methodology and observational data. Its ultimate purpose is to assist in the planning of future advanced studies for designing a mitigation plan for O_3 in Spain. To this end, relevant O_3 precursors, such as nitrogen oxides (NOx) and volatile organic compounds (VOCs), among other species, along with meteorological parameters associated with O_3, were analyzed from different data sources, including ground-level measurements and satellite observations, emissions inventory estimates, and meteorological reanalysis datasets.

The O_3 hotspots with the most opposing behaviors regarding O_3 trends were, at both ends, the Madrid area and the city of Sevilla. These act as both emissions sources of O_3 precursors and receptor areas. Madrid is impacted mainly by its own emissions, whereas Sevilla is affected by a large petrochemical area located downwind, while also contributes to the emission of pollutants that impact the interior of the Guadalquivir Valley (Querol et al. 2016 and references therein). The results suggest that, in the Madrid area, the generalized increasing O_3 trends may be mostly driven by major NOx decreases attributed to the road transport sector in this urban VOC-limited environment. Additionally, and to a lesser extent, an increase in surface temperature and other variations in meteorological parameters conducive to O_3 production may be at play. Conversely, the generalized decreasing O_3 trends in Sevilla city probably resulted from declining NOx emissions in a peculiar urban NOx-limited regime caused by AVOC contributions from a large petrochemical area located upwind (Diéguez et al. 2009), and increases in BVOCs associated with increased agricultural emissions and favorable meteorological conditions.

The other O_3 hotspots, including the interior of the Guadalquivir Valley, areas north of Barcelona, the closed Puertollano Basin, and the interior of the Valencian Community are receptor areas (located downwind of major emissions sources). Notably none of these areas exhibited O_3 trends, except for the interior of the Valencian Community, which displayed a less evident pattern. All of these hotspots are partly or entirely impacted by industrial, or other sector, emissions, apart from those from the road transport sector, as opposed to the Madrid area, where this is the primary contributor. The absence of clear trends in emissions from sectors other than road transport, and in some cases, increased emissions from specific sectors and precursors (possibly linked to the economic recovery following the 2008 financial crisis), coupled with the absence of significant meteorological variations conducive to O_3 production, seem to have contributed to the overall stability of O_3 concentrations in these hotspots.

Furthermore, in all the urban areas analyzed here, with the exception of Puertollano, surface NOx decreases attributed to the road transport sector and increases in O_3 (especially in the lower part of the O_3 distribution) were detected for the study period, pointing to a decrease in the titration effect as the main cause of these O_3 variations.

The findings from this study show that the parameters influencing O_3 vary distinctively across the different Spanish atmospheric regions—or O_3 hotspots—and that the causes underlying the contrasting O_3 trends differ significantly. This emphasizes the necessity of adopting an independent regional/local approach in planning O_3 mitigation measures.

In this study, we relied on satellite-based observations of formaldehyde (HCHO) as a proxy for VOCs emissions. However, the utility of these measurements in relation to O_3 is limited due to the presence of noise, low data frequency, and the fact that HCHO can be either primary or secondary. To improve on the available information, VOCs measurements with high temporal resolution, NOx/VOC sensitivity studies using both experimental and modeling methods, and higher disaggregation and temporal resolution in the VOCs and NOx

inventories are required. We believe that future studies should pursue these directions to advance our understanding of the complex relationships between O_3 and its precursors.

Supplementary Information The online version contains supplementary material available at https://doi.org/10.1007/s11869-023-01468-0.

Author contribution JM: conceptualization, data curation, formal analysis, investigation, methodology, software, validation, visualization, writing—original draft, writing—review and editing.

ME: conceptualization, formal analysis, investigation, methodology, validation, supervision, visualization, writing—original draft, writing—review and editing.

AA: formal analysis, funding acquisition, investigation, methodology, project administration, resources, supervision, validation, visualization, writing—review and editing.

EM: formal analysis, investigation, methodology, supervision, validation, visualization, writing—review and editing.

GG: formal analysis, investigation, methodology, supervision, validation, visualization, writing—review and editing.

HP: formal analysis, investigation, methodology, supervision, validation, visualization, writing—original draft, writing—review and editing.

CPGP: formal analysis, investigation, methodology, supervision, validation, visualization, writing—review and editing.

XQ: conceptualization, formal analysis, funding acquisition, investigation, methodology, project administration, resources, supervision, validation, visualization, writing—original draft, writing—review and editing.

Funding Open Access funding provided thanks to the CRUE-CSIC agreement with Springer Nature. The present work was supported by the Spanish Ministry of Ecological Transition and Demographic Challenge (Spanish National Ozone Plan); European Union's Horizon 2020 research and innovation program under grant agreement; the "Agencia Estatal de Investigación," from the Spanish Ministry of Science and Innovation, and FEDER funds under the project CAIAC (PID2019-108990RB-I00); the Generalitat de Catalunya (AGAUR 2021 SGR 00447); and the Ministerio de Ciencia e Innovación through the MITIGATE project (grant no. PID2020-113840RA-I00 funded by MCIN/AEI/10.13039/501100011033). This work was also supported by the Autonomous Government of Valencia (GVA) through the Valencian Institute for Business Competitiveness (IVACE) by means of the project Gaia (IMAMCA/2022/1). Carlos Pérez García-Pando acknowledges the support of the AXA Research Fund. We would like to thank NASA and the QA4ECV project for providing satellite-based data and the Climate Data Store (CDS) from the Copernicus Program for the ERA5 meteorological data.

Data availability The authors declare that the data supporting the findings of this study are available within the paper and its supplementary information files.

Declarations

Competing interests The authors declare no competing interests.

References

Abdi AM, Boke-Olén N, Jin H, Eklundh L, Tagesson T, Lehsten V, Ardö J (2019) First assessment of the plant phenology index (PPI) for estimating gross primary productivity in African semi-arid ecosystems. Int J Appl Earth Obs Geoinf 78:249–260

Archibald AT et al (2020) Tropospheric Ozone Assessment Report: a critical review of changes in the tropospheric ozone burden and budget from 1850 to 2100. Elem Sci Anth 8:1. https://doi.org/10.1525/elementa.2020.034

Azorin-Molina C, Guijarro JA, McVicar TR, Vicente-Serrano SM, Chen DL, Jerez S, Espirito-Santo F (2016) Trends of daily peak wind gusts in Spain and Portugal, 1961–2014. J Geophys Res Atmos. https://doi.org/10.1002/2015JD024485

Bechle MJ, Millet DB, Marshall JD (2013) Remote sensing of exposure to NO2: satellite versus ground-based measurement in a large urban area. Atmos Environ 69:345–353. https://doi.org/10.1016/j.atmosenv.2012.11.046,2013

Boersma KF, Eskes H, Richter A, De Smedt I, Lorente A, Beirle S, van Geffen J, Peters E, van Roozendael M, Wagner T (2017) QA4ECV NO2 tropospheric and stratospheric vertical column data from OMI (version 1.1) (Royal Netherlands Meteorological Institute (KNMI)). https://doi.org/10.21944/qa4ecv-no2-omi-v1.1. Accessed 13 Nov 2023

Borge R, Lumbreras J, Pérez J, de la Paz D, Vedrenne M, de Andrés JM, Rodríguez ME (2014) Emission inventories and modeling requirements for the development of air quality plans. Application to Madrid (Spain). Sci Total Environ 466–467:809–819. https://doi.org/10.1016/j.scitotenv.2013.07.093

Borge R, Weeberj JR, Yagüe C, Jhun I, Koutrakis P (2019) Impact of weather changes on air quality and related mortality in Spain over a 25 year period [1993–2017]. Environ Int 133(Part B):105272. https://doi.org/10.1016/j.envint.2019.105272

Byers L, Friedrich J, Hennig R et al (2021) A global database of power plants. World Resources Institute, Washington, DC. https://www.wri.org/research/global-database-power-plants. Accessed 13 Nov 2023

Carslaw D, Ropkins K (2012) Openair – an R package for air quality data analysis. Environ Model Softw 27–28:52–61

Castellanos P, Boersma K (2012) Reductions in nitrogen oxides over Europe driven by environmental policy and economic recession. Sci Rep 2:265. https://doi.org/10.1038/srep00265

Coates J, Mar KA, Ojha N, Butler TM (2016) The influence of temperature on ozone production under varying NO_x conditions – a modelling study. Atmos Chem Phys 16:11601–11615. https://doi.org/10.5194/acp-16-11601-2016

Colette A, Aas W, Banin L, Braban CF, Ferm M et al (2016) Air pollution trends in the EMEP region between 1990 and 2012. Joint Report of the EMEP Task Force on Measurements and Modelling (TFMM), Chemical Co-ordinating Centre (CCC), Meteorological Synthesizing Centre-East (MSC-E), Meteorological Synthesizing Centre-West (MSC-W). EMEP: TFMM/CCC/MSC-E/MSC-W Trend Report (01/2016). https://unece.org/environment-policy/publications/air-pollution-trends-emep-region-between-1990-and-2012. Accessed 13 Nov 2023

Cuevas C, Notario A, Adame J et al (2014) Evolution of NO2 levels in Spain from 1996 to 2012. Sci Rep 4:5887. https://doi.org/10.1038/srep05887

De Smedt I et al (2018) Algorithm theoretical baseline for formaldehyde retrievals from S5P TROPOMI and from the QA4ECV Project Atmos. Meas Tech 11:2395–2426

Diéguez JJ, Millán M, Padilla L, Palau JL (2009) Estudio y evaluación de la contaminación atmosférica por ozono troposférico en España, CEAM Report for the Ministry of Agriculture, Food and Environment, INF FIN/O3/2009, 372. https://www.miteco.gob.es/content/dam/miteco/es/calidad-y-evaluacion-ambiental/temas/atmosfera-y-calidad-del-aire/8_A_Informe%20final%20ozono-ceam%20Julio%202009_tcm30-188048.pdf. Accessed 13 Nov 2023

Diéguez JJ, Calatayud V, Mantilla E (2014) Informe Final, Memoria Técnica Proyecto CONOZE, CONtaminacióon por OZono en España, CEAM Report for the Ministry of Agriculture, Food and Environment, Fundación Biodiversidad, p 137. https://www.miteco.gob.es/es/calidad-y-evaluacion-ambiental/temas/atmosfera-y-calidad-del-aire/Informe_técnico_CONOZE-1-_tcm30-187899.pdf

EC (2008) Directive 2008/50/EC, of the European parliament and of the council of 21 May 2008 on ambient air quality and cleaner air for Europe http://data.europa.eu/eli/dir/2008/50/oj. Accessed 13 Nov 2023

EEA (2020) Air quality in Europe–2020 report, European Environment Agency. EEA Report, No 09/2020 (ISSN 1977–8449), 160. https://doi.org/10.2800/786656. Accessed 13 Nov 2023

EEA (2021a) Status report of air quality in Europe for year 2020. Eionet Report – ETC/ATNI 2021/8. https://www.eea.europa.eu/publications/air-quality-in-europe-2020-report. Accessed 13 November 2023

EEA (2021b) National emissions reported to the convention on long-range transboundary air pollution (LRTAP convention). https://www.eea.europa.eu/data-and-maps/dashboards/air-pollutant-emissions-data-viewer-4. Accessed 13 Nov 2023

EEA (2021c) EEA greenhouse gases - data viewer. Data viewer on greenhouse gas emissions and removals, sent by countries to UNFCCC and the EU Greenhouse Gas Monitoring Mechanism (EU Member States). https://www.eea.europa.eu/data-and-maps/data/data-viewers/greenhouse-gases-viewer. Accessed 13 Nov 2023

EEA (2022) European Union emission inventory report 1990–2020 under the UNECE air convention. EEA Report, No 03/2022 (ISBN 978–92–9480–487–7), 160. https://doi.org/10.2800/928370. Accessed 13 Nov 2023

ESA (2021) Satellites detect large methane emissions from Madrid landfills. ESA Applications. Observing the Earth. https://www.esa.int/Applications/Observing_the_Earth/Satellites_detect_large_methane_emissions_from_Madrid_landfills. Accessed 13 Nov 2023

Escudero M, Segers A, Kranenburg R, Querol X, Alastuey A, Borge R, de la Paz D, Gangoiti G, Schaap M (2019) Analysis of summer O3 in the Madrid air basin with the LOTOS-EUROS chemical transport model. Atmos Chem Phys 19:14211–14232. https://doi.org/10.5194/acp-19-14211-2019

Fleming ZL, Doherty RM, von Schneidemesser E, Malley CS, Cooper OR, Pinto JP, Colette A, Xu X, Simpson D, Schultz MG, Lefohn AS, Hamad S, Moolla R, Solberg S, Feng Z (2018) Tropospheric Ozone Assessment Report: present-day ozone distribution and trends relevant to human health. Elem Sci Anth 6(1):12. https://doi.org/10.1525/elementa.273

Fowler D, Pilegaard K, Sutton MA, Ambus P, Raivonen M, Duyzer J, Simpson D, Fagerli H, Fuzzi S, Schjoerring JK, Granier C, Neftel A, Isaksen ISA, Laj P, Maione M, Monks PS, Burkhardt J, Daemmgen U, Neirynck J, Personne E, Wichink-Kruit R et al (2009) Atmospheric composition change: ecosystems-atmosphere interactions. Atmos Environ 43:5193–5267. https://doi.org/10.1016/j.atmosenv.2009.07.068

Gangoiti G, Millán MM, Salvador R, Mantilla E (2001) Long-range transport and re-circulation of pollutants in the western Mediterranean during the project Regional Cycles of Air Pollution in the West-Central Mediterranean Area. Atmos Environ 35:6267–6276. https://doi.org/10.1016/S1352-2310(01)00440-X

Gangoiti G, Alonso L, Navazo M, Albizuri A, Perez-Landa G, Matabuena M, Valdenebro V, Maruri M, García JA, Millán MM (2002) Regional transport of pollutants over the Bay of Biscay: analysis of an ozone episode under a blocking anticyclone in west-central Europe. Atmos Environ 36(8):1349–1361. https://doi.org/10.1016/S1352-2310(01)00536-2

Gangoiti G, Albizuri A, Alonso L, Navazo M, Matabuena M, Valdenebro V, García JA, Millán MM (2006) Sub-continental transport mechanisms and pathways during two ozone episodes in northern Spain. Atmos Chem Phys 6:1469–1484

Garrido-Perez JM, Ordóñez C, García-Herrera R, Barriopedro D (2018) Air stagnation in Europe: spatiotemporal variability and impact on air quality. Sci Total Environ 645:1238–1252. https://doi.org/10.1016/j.scitotenv.2018.07.238

Garrido-Perez JM, Ordóñez C, García-Herrera R, Schnell JR (2019) The differing impact of air stagnation on summer ozone across Europe. Atmos Environ 219:117062. https://doi.org/10.1016/j.atmosenv.2019.117062. (ISSN 1352-2310)

Gaudel A, Cooper OR, Ancellet G et al (2018) Tropospheric Ozone Assessment Report: present-day distribution and trends of tropospheric ozone relevant to climate and global atmospheric chemistry model evaluation. Elementa: Sci Anthropocene 6:39. https://doi.org/10.1525/elementa.291

GBD (2016) Global burden of disease study 2016 cause-specific mortality 1980–2016 Seattle, United States: Institute for Health Metrics and Evaluation (IHME). https://ghdx.healthdata.org/record/ihme-data/gbd-2016-cause-specific-mortality-1980-2016. Accessed 13 Nov 2023

Guenther A, Hewitt C, Erickson D, Fall R, Geron C, Graedel T, Harley P, Klinger L, Lerdau M, McKay W, Pierce T, Scholes R, Steinbrecher R, Tallamraju R, Taylor J, Zimmerman P (1995) A global model of natural volatile organic compound emissions. J Geophys Res 100:8873–8892

Guevara M, Pay MT, Martínez F, Soret A, Denier van der Gon H, Baldasano JM (2014) Inter-comparison between HERMESv2.0 and TNO-MACC-II emission data using the CALIOPE air quality system (Spain). Atmos Environ 98:134–145. https://doi.org/10.1016/j.atmosenv.2014.08.067

Guevara M, Petetin H, Jorba O, Denier van der Gon H, Kuenen J, Super I, Jalkanen JP, Majamaki E, Johansson L, Peuch VH, Pérez García-Pando C (2022) European primary emissions of criteria pollutants and greenhouse gases in 2020 modulated by the COVID-19 pandemic disruptions. Earth Syst Sci Data 14:2521–2552. https://doi.org/10.5194/essd-14-2521-2022

Hersbach H, Bell B, Berrisford P, Biavati G, Horányi A, Muñoz Sabater J, Nicolas J, Peubey C, Radu R, Rozum I, Schepers D, Simmons A, Soci C, Dee D, Thépaut J-N (2019) ERA5 monthly averaged data on single levels from 1959 to present. Copernicus Clim Chang Serv (C3S) Clim Data Store (CDS). https://doi.org/10.24381/cds.f17050d7

In 't Veld M, Carnerero C, Massagué J, Alastuey A, de la Rosa J, Sánchez AM, Escudero M, Mantilla E, Gangoiti G, Pérez C, Olid M, Moreta JR, Hernández JL, Santamaría J, Millán M, Querol X (2021) Understanding the local and remote source contributions to ambient O3 during a pollution episode using a combination of experimental approaches in the Guadalquivir Valley, Southern Spain. Sci Total Environ 777:144579. https://doi.org/10.1016/j.scitotenv.2020.144579

INE (2022) Statistics about territories. Instituto Nacional de Estadística (National Statistics Institute). ISSN: 2792-9582. https://www.ine.es/dynInfo/Infografia/Territoriales/en/index.html. Accessed 13 November 2023.

IPCC (2021) Climate change 2021: the physical science basis. Contribution of working group I to the sixth assessment report of the intergovernmental panel on climate change. In: Masson-Delmotte V, Zhai P, Pirani A, Connors SL, Péan C, Berger S, Caud N, Chen Y, Goldfarb L, Gomis MI, Huang M, Leitzell K, Lonnoy E, Matthews JBR, Maycock TK, Waterfield T, Yelekçi O, Yu R, Zhou B (eds) Cambridge University Press, Cambridge and New York, NY, p 2391.https://doi.org/10.1017/9781009157896

Jacob D, Winner D (2009) Effect of climate change on air quality. Atmos Environ 43(1):51–63

Jacob D, Horowitz LW, Munger W, Heikes BG, Dickerson R et al (1995) Seasonal transition from NOx to hydrocarbon-limited conditions for ozone production over the eastern United States in September. J Geophys Res 100:9315–9324. https://doi.org/10.1029/94JD03125

Jonson JE, Schulz M, Emmons L, Flemming J, Henze D, Sudo K, Tronstad Lund M, Lin M, Benedictow A, Koffi B, Dentener F, Keating T, Kivi R, Davila Y (2018) The effects of intercontinental emission sources on European air pollution levels. Atmos Chem Phys 18:13655–13672. https://doi.org/10.5194/acp-18-13655-2018

Jonson JE, Gauss M, Schulz M, Jalkanen J-P, Fagerli H (2020) Effects of global ship emissions on European air pollution levels. Atmos Chem Phys 20:11399–11422. https://doi.org/10.5194/acp-20-11399-2020

Langner J, Engardt M, Andersson C (2012) European summer surface ozone 1990–2100. Atmos Chem Phys 12:10097–10105. https://doi.org/10.5194/acp-12-10097-2012

Lefohn AS, Malley CS, Simon H, Wells B, Xu X et al (2017) Responses of human health and vegetation exposure metrics to changes in ozone concentration distributions in the European Union, United States, and China. Atmos Environ 152:123–145. https://doi.org/10.1016/j.atmosenv.2016.12.025

Lefohn AS, Malley CS, Smith L, Wells B, Hazucha M, Simon H, Naik V, Mills G, Schultz MG et al (2018) Tropospheric Ozone Assessment Report: global ozone metrics for climate change, human health, and crop/ecosystem research. Elem Sci Anth 6:28. https://doi.org/10.1525/elementa.279

Li D, Wang S, Xue R, Zhu J, Zhang S, Sun Z, Zhou B (2021) OMI-observed HCHO in Shanghai, China, during 2010–2019 and ozone sensitivity inferred by an improved HCHO / NO2 ratio. Atmos Chem Phys 21:15447–15460. https://doi.org/10.5194/acp-21-15447-2021

Liu F, Beirle S, Zhang Q, Dörner S, He K, Wagner T (2016) NOx lifetimes and emissions of cities and power plants in polluted background estimated by satellite observations. Atmos Chem Phys 16:5283–5298. https://doi.org/10.5194/acp-16-5283-2016

Martin RV, Fiore AM, Van Donkelaar A (2004) Space-based diagnosis of surface ozone sensitivity to anthropogenic emissions. Geophys Res Lett 31:L06120. https://doi.org/10.1029/2004GL019416

Massagué J, Carnerero C, Escudero M, Baldasano JM, Alastuey A, Querol X (2019) 2005–2017 ozone trends and potential benefits of local measures as deduced from air quality measurements in the north of the Barcelona metropolitan area. Atmos Chem Phys 19:7445–7465. https://doi.org/10.5194/acp-19-7445-2019

Massagué J, Contreras A, Campos A, Alastuey A, Querol X (2021) 2005–2018 trends in ozone peak concentrations and spatial contributions in the Guadalquivir Valley Southern Spain. Atmos Environ 254(22):118385. https://doi.org/10.1016/j.atmosenv.2021.118385

Massagué J, Escudero M, Alastuey A, Mantilla E, Monfort E, Gangoiti G, Pérez García-Pando C, Querol X (2023) Spatiotemporal variations of tropospheric ozone in Spain (2008–2019). Environ Int. https://doi.org/10.1016/j.envint.2023.107961. (ACCEPTED)

McLinden CA, Olsen SC, Hannegan B, Wild O, Prather MJ, Sundet J (2000) Stratospheric ozone in 3-D models: a simple chemistry and the cross-tropopause flux. J Geophys Res: Atmos 105:14653–14665. https://doi.org/10.1029/2000jd900124

Millán MM, Salvador R, Mantilla E, Kallos G (1997) Photooxidant dynamics in the Mediterranean basin in summer: results from European research projects. J Geophys Res 102:8811–8823

Millán MM, Mantilla E, Salvador R, Carratalá A, Sanz MJ, Alonso L, Gangoiti G, Navazo M (2000) Ozone cycles in the western Mediterranean Basin: interpretation of monitoring data in complex coastal terrain. J Appl Meteorol 39:487–508

Millán MM, Sanz MJ, Salvador R, Mantilla E (2002) Atmospheric dynamics and ozone cycles related to nitrogen deposition in the western Mediterranean. Environ Pollut 118:167–186

Mills G, Pleijel H, Malley C, Sinha B, Cooper OR, Schultz MG, Neufeld HS, Simpson D, Sharps K, Feng Z, Gerosa G, Harmens H, Kobayashi K, Saxena P, Paoletti E, Sinha V, Xu X, Helmig D, Lewis A (2018) Tropospheric Ozone Assessment Report: present-day tropospheric ozone distribution and trends relevant to vegetation. Sci Anthropocene 6:47. https://doi.org/10.1525/elementa.302

Minguillón MC, Monfort E, Escrig A, Celades I, Guerra L et al (2013) Air quality comparison between two European ceramic tile clusters. Atmos Environ 74:311–319

MITERD (2023) Inventory informative report (on Pollutant Emissions). Submission to the secretariat of the Geneva Convention and EMEP Programme. Reporting to the European commission under directive (EU) 2016/2284. 2023 EDITION (1990–2021). https://cdr.eionet.europa.eu/es/un/clrtap/iir/envzbfuja/IIR_2023_ES.pdf/manage_document. Accessed 13 Nov 2023

Monks PS, Archibald AT, Colette A, Cooper O, Coyle M, Derwent R, Fowler D, Granier C, Law KS, Mills GE, Stevenson DS, Tarasova O, Thouret V, von Schneidemesser E, Sommariva R, Wild O, Williams ML (2015) Tropospheric ozone and its precursors from the urban to the global scale from air quality to short-lived climate forcer. Atmos Chem Phys 15:8889–8973

Myhre Gunnar, Shindell Drew, Pongratz Julia (2014) Anthropogenic and Natural Radiative Forcing. In: Stocker Thomas (ed) Climate change 2013: the physical science basis; Working Group I contribution to the fifth assessment report of the Intergovernmental Panel on Climate Change. Cambridge University Press, Cambridge, pp 659–740

Notario A, Bravo I, Adame JA, Díaz-de-Mera Y, Aranda A, Rodríguez A, Rodríguez D (2012) Analysis of NO, NO2, NOx, O3 and oxidant (Ox=O3+NO2) levels measured in a metropolitan area in the southwest of Iberian Peninsula. Atmos Res 104–105(2):217–226. https://doi.org/10.1016/j.atmosres.2011.10.008

Notario A, Bravo I, Adame JA et al (2013) Behaviour and variability of local and regional oxidant levels ($OX = O_3 + NO_2$) measured in a polluted area in central-southern of Iberian Peninsula. Environ Sci Pollut Res 20:188–200. https://doi.org/10.1007/s11356-012-0974-1,2013

Nunes RAO, Alvim-Ferraz MCM, Martins FG, Calderay-Cayetano F, Durán-Grados V, Moreno-Gutiérrez J, Jalkanen J-P, Hannuniemi H, Sousa SIV (2020) Shipping emissions in the Iberian Peninsula and the impacts on air quality. Atmos Chem Phys 20:9473–9489. https://doi.org/10.5194/acp-20-9473-2020

Oliveira K, Guevara M, Jorba O, Querol X, García-Pando CP (2023) A new NMVOC speciated inventory for a reactivity-based approach to support ozone control strategies in Spain. Sci Total Environ 867:161449

Olson JR, Crawford JH, Davis DD, Chen G, Avery MA, Barrick JDW, Sachse GW, Vay SA, Sandholm ST, Tan D, Brune WH, Faloona IC, Heikes BG, Shetter RE, Lefer BL, Singh HB, Talbot RW, Blake DR (2001) Seasonal differences in the photochemistry of the South Pacific: a comparison of observations

and model results from PEM-tropics A and B. J Geophys Res 106:32749–32766

OMI Team (2012) Ozone monitoring instrument (OMI) data user's guide. https://docserver.gesdisc.eosdis.nasa.gov/repository/Mission/OMI/3.3_ScienceDataProductDocumentation/3.3.2_ProductRequirements_Designs/README.OMI_DUG.pdf. Accessed Nov 2023

Opacka B, Müller J-F, Stavrakou T, Bauwens M, Sindelarova K, Markova J, Guenther AB (2021) Global and regional impacts of land cover changes on isoprene emissions derived from spaceborne data and the MEGAN model. Atmos Chem Phys 21:8413–8436. https://doi.org/10.5194/acp-21-8413-2021

Otero N, Sillmann J, Schnell JL, Rust HW, Butler T (2016) Synoptic and meteorological drivers of extreme ozone concentrations over Europe. Environ Res Lett 11:24005. https://doi.org/10.1088/1748-9326/11/2/024005

Pacca L, Antonarakis A, Schröder P, Antoniades A (2020) The effect of financial crises on air pollutant emissions: an assessment of the short vs. medium-term effects. Sci Total Environ 698:133614

Paoletti E, De Marco A, Beddows DCS, Harrison RM, Manning WJ (2014) Ozone levels in European and USA cities are increasing more than at rural sites, while peak values are decreasing. Environ Pollut 192:295–299. https://doi.org/10.1016/j.envpol.2014.04.040

Peters GP, Gregg M, Le Quere C, Boden TA, Canadell J, Raupach M (2011) Rapid growth in CO2 emissions after the 2008-2009 global financial crisis, United States. https://doi.org/10.1038/nclimate1332

Pfeifroth U, Sanchez-Lorenzo A, Manara V, Trentmann J, Hollmann R (2018) Trends and variability of surface solar radiation in Europe based on surface- and satellite-based data records. J Geophys Res: Atmos 123:1735–1754. https://doi.org/10.1002/2017JD027418

Plaza J, Pujadas M, Artíñano B (1997) Formation and transport of the Madrid ozone plume. JAPCA J Air Waste Ma 47:766–774

Porter WC, Heald CL (2019) The mechanisms and meteorological drivers of the summertime ozone–temperature relationship. Atmos Chem Phys 19:13367–13381. https://doi.org/10.5194/acp-19-13367-2019

Puertos del Estado (2022) Annual statistical report of the state-owned port system. Ministerio de Transportes, Movilidad y Agenda Urbana. https://www.puertos.es/es-es/estadisticas/Paginas/CuadroMando_anual.aspx. Accessed 13 Nov 2023

Pusede SE, Steiner AL, Cohen RC (2015) Temperature and recent trends in the chemistry of continental surface, 790 ozone. Chem Rev 115:3898–3918. https://doi.org/10.1021/cr5006815

Querol X, Alastuey A, Orio A, Pallares M, Reina F, Diéguez JJ, Mantilla E, Escudero M, Alonso L, Gangoiti G, Millán M (2016) On the origin of the highest ozone episodes in Spain. Sci Total Environ 572:379–389

Querol X, Gangoiti G, Mantilla E, Alastuey A, Minguillón MC, Amato F, Reche C, Viana M, Moreno T, Karanasiou A, Rivas I, Pérez N, Ripoll A, Brines M, Ealo M, Pandolfi M, Lee H-K, Eun H-R, Park Y-H, Escudero M, Beddows D, Harrison RM, Bertrand A, Marchand N, Lyasota A, Codina B, Olid M, Udina M, Jiménez-Esteve B, Soler MR, Alonso L, Millán M, Ahn K-H (2017) Phenomenology of high-ozone episodes in NE Spain. Atmos Chem Phys 17:2817–2838

Querol X, Alastuey A, Gangoiti G, Perez N, Lee HK, Eun HR, Park Y, Mantilla E, Escudero M, Titos G, Alonso L, Temime-Roussel B, Marchand N, Moreta JR, Revuelta MA, Salvador P, Artíñano B, García dos Santos S, Anguas M, Notario A, Saiz-Lopez A, Harrison RM, Millán M, Ahn K-H (2018) Phenomenology of summer ozone episodes over the Madrid Metropolitan Area, central Spain. Atmos Chem Phys 18:6511–6533. https://doi.org/10.5194/acp-18-6511-2018

Querol X, Massagué J, Alastuey A, Moreno T, Gangoiti G, Mantilla E, Diéguez JJ, Escudero M, Monfort E, García-Pando CP et al (2021) Lessons from the COVID-19 air pollution decrease in Spain: now what? Sci Total Environ 779:146380

R Core Team (2021) R: a language and environment for statistical computing. R Foundation for Statistical Computing. Vienna, Austria. https://www.R-project.org. Accessed 13 Nov 2023

Reche C, Moreno T, Amato F, Pandolfi M, Pérez J, de la Paz D et al (2018) Spatio-temporal patterns of high summer ozone events in the Madrid Basin, Central Spain. Atmos Environ 185:207–220. https://doi.org/10.1016/j.atmosenv.2018.05.002

REE (2021) The Spanish electricity system report. Preliminary report 2021. Red Eléctrica de España. Publications. https://www.ree.es/en/datos/publications/annual-system-report. Accessed 13 Nov 2023

Rubin JI, Kean AJ, Harley RA, Millet DB, Goldstein AH (2006) Temperature dependence of volatile organic compound evaporative emissions from motor vehicles. J Geophys Res-Atmos 111:d03305. https://doi.org/10.1029/2005JD006458

Saavedra S, Rodríguez A, Taboada JJ, Souto JA, Souto JA (2012) Synoptic patterns and air mass transport during ozone episodes in northwestern Iberia. Sci Total Environ 441:97–110. https://doi.org/10.1016/j.scitotenv.2012.09.014

Saiz-Lopez A, Adame JA, Notario A, Poblete J, Bolívar JP, Albaladejo J (2009) Year-round observations of NO, NO2, O3, SO2, and toluene measured with a DOAS system in the industrial area of Puertollano, Spain. Water Air Soil Pollut 200:277–288. https://doi.org/10.1007/s11270-008-9912-8,2009

Saiz-Lopez A et al (2017) Unexpected increase in the oxidation capacity of the urban atmosphere of Madrid, Spain. Sci Rep 7:45956. https://doi.org/10.1038/srep45956

Sartelet KN, Couvidat F, Seigneur C, Roustan Y (2012) Impact of biogenic emissions on air quality over Europe and North America. Atmos Environ 53:131–141. https://doi.org/10.1016/j.atmosenv.2011.10.046. (aQMEII: An International Initiative for the Evaluation of Regional-Scale Air Quality Models Phase 1)

Saunois M, Stavert AR, Poulter B, Bousquet P, Canadell JG et al (2020) The global methane budget 2000–2017. Earth Syst Sci Data 12:1561–1623. https://doi.org/10.5194/essd-12-1561-2020

Sen PK (1968) Estimates of the regression coefficient based on Kendall's Tau. J Am Stat Assoc 63:1379–1389.https://doi.org/10.1080/01621459.1968.10480934

Sicard (2021) Ground-level ozone over time: an observation-based global overview. Curr Opin Environ Sci Health 19:100226. https://doi.org/10.1016/j.coesh.2020.100226. (ISSN 2468-5844)

Sicard P, De Marco A, Troussier F, Renou C, Vas N, Paoletti E (2013) Decrease in surface ozone concentrations at Mediterranean remote sites and increase in the cities. Atmos Environ 79:705–715

Sicard P, Serra R, Rossello P (2016) Spatio-temporal trends of surface ozone concentrations and metrics in France. Environ Res 149:122–144. https://doi.org/10.1016/j.envres.2016.05.014,2016

Sillman S (1999) The relation between ozone, NOx and hydrocarbons in urban and polluted rural environments. Atmos Environ 33:1821–1845. https://doi.org/10.1016/S1352-2310(98)00345-8

Sillman S, He D (2002) Some theoretical results concerning O3-NOx-VOC chemistry and NOx-VOC indicators. J Geophys Res 107(D22):4659. https://doi.org/10.1029/2001JD001123

Sillman S, Samson PJ (1995) Impact of temperature on oxidant photochemistry in urban, polluted rural and remote environments. J Geophys Res-Atmos 100:11497–11508

Sillman S, Vautard R, Menut L, Kley D (2003) O3-NOx-VOC sensitivity and NOx-VOC indicators in Paris: results from models and

Atmospheric Pollution Over the Paris Area (ESQUIF) measurements. J Geophys Res 108:8563. https://doi.org/10.1029/2002JD001561

Simon H, Reff A, Wells B, Xing J, Frank N (2015) Ozone trends across the United States over a period of decreasing NOx and VOC emissions. Environ Sci Technol 49:186–195. https://doi.org/10.1021/es504514z

Sokhi RS, Singh V, Querol X et al (2021) A global observational analysis to understand changes in air quality during exceptionally low anthropogenic emission conditions. Environ Int 157:106818. https://doi.org/10.1016/j.envint.2021.106818

Soret A, Guevara M, Baldasano JM (2014) The potential impacts of electric vehicles on air quality in the urban areas of – and Madrid (Spain). Atmos Environ 99:51–63. https://doi.org/10.1016/j.atmosenv.2014.09.048

Souri AH, Nowlan CR, Wolfe GM, Lamsal LN, Chan Miller CE, González Abad G et al (2020) Revisiting the effectiveness of HCHO/NO2 ratios for inferring ozone sensitivity to its precursors using high resolution airborne remote sensing observations in a high ozone episode during the KORUS-AQ campaign. Atmos Environ 224:117341. https://doi.org/10.1016/j.atmosenv.2020.117341. (ISSN 1352-2310)

Souri AH, Johnson MS, Wolfe GM, Crawford JH, Fried A, Wisthaler A et al (2022) Characterization of errors in satellite-based HCHO / NO_2 tropospheric column ratios with respect to chemistry, column to pbl translation, spatial representation, and retrieval uncertainties. Atmos Chem Phys Discuss [preprint]. https://doi.org/10.5194/acp-2022-410. (ISSN 1352-2310)

Stevenson DS, Dentener FJ, Schultz MG, Ellingsen K, van Noije TPC et al (2006) Multimodel ensemble simulations of present-day and near-future tropospheric ozone. J Geophys Res Atmos 111:D08301. https://doi.org/10.1029/2005jd006338

Targa T, Ripoll A, Banyuls L, González A, Soares J (2022) Status report of air quality in Europe for year 2021, using validated and up-to-date data (Eionet Report – ETC/HE, 2022/3). https://www.eionet.europa.eu/etcs/etc-he/products/etc-he-products/etc-he-reports/etc-he-report-2022-3-status-report-of-air-quality-in-europe-for-year-2021-using-validated-and-up-to-date-data. Accessed 13 Nov 2023

Theil H (1992) A rank-invariant method of linear and polynomial regression analysis. In: Raj B, Koerts J (eds) Henri Theil's contributions to economics and econometrics. Advanced Studies in Theoretical and Applied Econometrics, vol 23. Springer, Dordrecht. https://doi.org/10.1007/978-94-011-2546-8_20

Toll I, Baldasano JM (2000) Modeling of photochemical air pollution in the Barcelona area with highly disaggregated anthropogenic and biogenic emissions. Atmos Environ 34:1352–2310. https://doi.org/10.1016/S1352-2310(99)00498-7

Tu Q, Hase F, Schneider M, García O, Blumenstock T, Borsdorff T et al (2022) Quantification of CH4 emissions from waste disposal sites near the city of Madrid using ground- and space-based observations of COCCON, TROPOMI and IASI. Atmos Chem Phys 22:295–317. https://doi.org/10.5194/acp-22-295-2022

Turnock ST, Wild O, Dentener FJ, Davila Y, Emmons LK, Flemming J, Folberth GA, Henze DK, Jonson JE, Keating TJ, Kengo S, Lin M, Lund M, Tilmes S, O'Connor FM (2018) The impact of future emission policies on tropospheric ozone using a parameterised approach. Atmos Chem Phys 18:8953–8978. https://doi.org/10.5194/acp-18-8953-2018

Valverde V, Pay MT, Baldasano JM (2016) Ozone attributed to Madrid and Barcelona on-road transport emissions: characterization of plume dynamics over the Iberian Peninsula. Sci Total Environ 543:670–682

Van Dingenen R, Crippa M, Maenhout G, Guizzardi D, Dentener F (2018) Global trends of methane emissions and their impacts on ozone concentrations, EUR 29394 EN, Publications Office of the European Union, Luxembourg, 2018. https://data.europa.eu/doi/10.2760/820175

von Schneidemesser E, Monks PS, Allan JD, Bruhwiler L, Forster P et al (2015) Chemistry and the linkages between air quality and climate change. Chem Rev 115(10):3856–3897. https://doi.org/10.1021/acs.chemrev.5b00089

Wei J, Li Z, Dickerson R, Pinker R, Wang J, Liu X, Sun L, Xue W, Cribb M (2022) Full-coverage mapping and spatiotemporal variations of ground-level ozone (O3) pollution from 2013 to 2020 across China. Remote Sens Environ 270:112775. https://doi.org/10.1016/j.rse.2021.112775,2022

Weng H, Lin J, Martin R, Millet DB, Jaeglé L et al (2020) Global high-resolution emissions of soil NOx, sea salt aerosols, and biogenic volatile organic compounds. Sci Data 7:148. https://doi.org/10.1038/s41597-020-0488-5

WHO (2013a) Regional Office for Europe: Review of evidence on health aspects of air pollution—REVIHAAP project: technical report, WHO Regional Office for Europe, Copenhagen. WHO/EURO:2013-4101-43860-61757, p 302. https://www.who.int/europe/publications/i/item/WHO-EURO-2013-4101-43860-61757. Accessed 13 Nov 2023

WHO (2013b) Regional office for Europe: Health risks of air pollution in Europe–HRAPIE Project: recommendations for concentration-response functions for cost–benefit analysis of particulate matter, ozone and nitrogen dioxide, Copenhagen, p 65 pp. Available at: https://iris.who.int/handle/10665/153692?locale-attribute=fr&locale=ar2022. Accessed 13 Nov 2023

WHO (2021) Global air quality guidelines (2021) Particulate matter (PM2.5 and PM10), ozone, nitrogen dioxide, sulfur dioxide and carbon monoxide. Geneva: World Health Organization. https://www.who.int/publications/i/item/9789240034228. Accessed 13 Nov 2023

Wolfe GM, Kaiser J, Hanisco TF, Keutsch FN, de Gouw JA et al (2016) Formaldehyde production from isoprene oxidation across NOx regimes. Atmos Chem Phys 16:2597–2610. https://doi.org/10.5194/acp-16-2597-2016

Yan Y, Lin J, Pozzer A, Kong S, Lelieveld J (2019) Trend reversal from high-to-low and from rural-to-urban ozone concentrations over Europe. Atmos Environ 213:25–36

Young PJ, Archibald AT, Bowman KW, Lamarque J-F, Naik V, Stevenson DS et al (2013) Preindustrial to end 21st century projections of tropospheric ozone from the Atmospheric Chemistry and Climate Model Intercomparison Project (ACCMIP). Atmos Chem Phys 13:2063–2090. https://doi.org/10.5194/acp-13-2063-2013